Acta Biomaterialia 151 (2022) 235–253

Contents lists available at ScienceDirect

Acta Biomaterialia

journal homepage: www.elsevier.com/locate/actbio

Full length article

Hofmeister effect-enhanced gelatin/oxidized dextran hydrogels with improved mechanical properties and biocompatibility for wound healing

Binan Zhao[a,1], Yuanzhen Zhang[a,1], Dandan Li[b,1], Xiumei Mo[b,*], Jianfeng Pan[a,*]

[a] Department of Orthopedics, Shanghai Tenth People's Hospital, School of Medicine, Tongji University, 301 Yanchang Road, Shanghai 200072, China
[b] State Key Laboratory for Modification of Chemical Fibers and Polymer Materials, Shanghai Engineering Research Center of Nano-Biomaterials and Regenerative Medicine, College of Biological Science and Medical Engineering, Donghua University, Shanghai 201620, China

ARTICLE INFO

Article history:
Received 26 April 2022
Revised 3 August 2022
Accepted 4 August 2022
Available online 9 August 2022

Keywords:
Hofmeister effect
Schiff base
Hydrogel
Gelatin
Mechanical stability
Biocompatibility

ABSTRACT

Compared with other types of hydrogels, natural derived hydrogels possess intrinsic advantages of degradability and biocompatibility. However, due to the low mechanical strength, their potential applications in biomedical areas are limited. In this study, Hofmeister effect-enhanced gelatin/oxidized dextran (Gel/O-Dex) hydrogels were designed with improved mechanical properties and biocompatibility to accelerate wound healing. Gel and O-Dex were chemically crosslinked through Schiff base reaction of aldehyde and amino groups. After soaking in kosmotrope solutions physical crosslinking domains were induced by Hofmeister effect including α-helix structures, hydrophobic interaction regions and helical junction zones among Gel molecular chains. The type of anions played different influence on the properties of hydrogels, which was consistent with the order of Hofmeister series. Particularly, $H_2PO_4^-$ treated hydrogels showed enhanced mechanical strength and fatigue resistance superior to that of Gel/O-Dex hydrogels. The underlying mechanism was that the physical crosslinking domains sustained additional mechanical stress and dissipated energy through cyclic association and dissociation process. Furthermore, Hofmeister effect only induced polymer chain entanglements without triggering any chemical reaction. Due to Hofmeister effect of $H_2PO_4^-$ ions, aldehyde groups were embedded in the center of entangled polymer chains that resulted in better biocompatibility. In the full-thickness skin defects of SD rats, Hofmeister effect-enhanced Gel/O-Dex hydrogels by $H_2PO_4^-$ ions accelerated wound healing and exhibited better histological morphology than ordinary hydrogels. Therefore, Hofmeister effect by essential inorganic anions is a promising method of improving mechanical properties and biocompatibility of natural hydrogels to promote medical translation in the field of wound healing from bench to clinic.

Statement of significance

Hofmeister effect enhanced hydrogel mechanical properties in accordance with the order of Hofmeister series through physical crosslinking that induced α-helix structures, hydrophobic interaction regions and helical junction zones among Gel molecular chains. Due to the Hofmeister effect of $H_2PO_4^-$ ions, aldehyde groups were embedded in the center of entangled polymer chains that resulted in better biocompatibility. Hofmeister effect-enhanced Gel/O-Dex hydrogels through $H_2PO_4^-$ ions accelerated wound healing and exhibited better histological morphology than ordinary hydrogels. Therefore, Hofmeister effect by essential inorganic anions is a promising method to improve mechanical properties and biocompatibility of natural hydrogels for their medical applications..

1. Introduction

Hydrogels are water-swollen polymeric matrices formed by chemical crosslinking of covalent bonds or physical crosslinks from entanglements and interactions between polymer chains [1,2]. Due to their capacity of high water content, hydrogels are widely used in tissue engineering to simulate physiological environments and

* Corresponding authors.
E-mail addresses: xmm@dhu.edu.cn (X. Mo), jianfengpan@tongji.edu.cn (J. Pan).
[1] These authors contributed equally to this work.

https://doi.org/10.1016/j.actbio.2022.08.009
1742-7061/

facilitate tissue regeneration. Depending on the material source of fabrication, hydrogels can be classified into three categories: (i) natural derived hydrogels, (ii) synthetic hydrogels, and (iii) natural-synthetic copolymer hydrogels. Synthetic and natural-synthetic copolymer hydrogels can be prepared with precisely controlled structures and generally exhibit exceptional mechanical properties. However, they will not be completely degraded into human body's natural metabolites through simple degradation under physiological conditions. The problems of biocompatibility and irritation of inflammatory reaction are still under close concern due to the use of toxic chemicals in their synthesis or processing [3]. In contrast, natural hydrogels that are derived from natural polymers, usually exhibit potential advantages of biocompatibility and biodegradation. These hydrogels offer the possibility to create completely natural tissue or organ equivalents since they are composed of naturally occurring substances. They can be produced from absorbable natural materials such as gelatin, collagen, alginate, hyaluronate and dextran polymers. The unfavorable problems of synthetic or natural-synthetic hydrogels may thereby be suppressed. Generally, natural hydrogels are more complicated in structure than most synthetic hydrogels and the technical manipulation is also more elaborate. Therefore, we focus our research efforts on natural hydrogels and their chemically-physically modified versions to provide an unprecedented solution.

Because the application range of natural hydrogels is severely limited by their mechanical properties, the critical challenge nowadays is how to improve their mechanical strength. This is critical for implanting them into the body to replace native tissue and integrating them with the rest of the body, as the natural hydrogels must create and maintain a space for tissue development. Additionally, the mechanical properties of hydrogels are also tightly associated with the adhesion and gene expression of cells [4]. Previous work has demonstrated that the mechanical properties of hydrogels mainly depend on the types of crosslinked polymer molecules, the original rigidity of polymer chains, the swelling of hydrophilic/hydrophobic balance and crosslinking density [5]. In the past few years, several strategies have been proposed to improve the mechanical strength of natural polymer hydrogels including multiple gelation methodologies and nano-reinforced approaches doped with various nanoscale fillers [6,7]. By using chemical and physical crosslinking in tandem, double-network structure was introduced to increase the crosslinking sites between polymers and the resultant modified hydrogels showed improved mechanical properties compared to their original state [8]. Nevertheless, the multiple gelation methodologies typically require more cumbersome processes designed to impart mechanical behaviors, which may impede the optimization of other functions. Also, other hybrid hydrogels comprising phyllosilicate nanoplatelets or ultralong hydroxyapatite nanowires were prepared to provide mechanical reinforcement [9,10]. The interesting nanofillers required in the reinforced hydrogels may play an appreciable impact on the performance of the scaffold material, thereby compromising other desired properties. Thus, a substantial need exists for natural polymer hydrogels that improve the mechanical performance via a simple and straightforward strategy without sacrificing the convenience of handling and the simplicity of manipulation.

Recently, Hofmeister effect-assisted gelatin hydrogels were fabricated to obtain ductile and strong mechanical properties. Highly kosmotropic ions were proven to greatly enhance the chain bundling and hydrophobic interactions via Hofmeister effect so that extraordinary mechanical strength was achieved in kosmotropic ions induced gelatin gels [11]. The Hofmeister series was introduced by Hofmeister in 1888, in which a series of experiments were conducted to rank various salts according to their ability to precipitate egg white proteins in aqueous solutions. Since then, the effect of ions on protein stability has been called Hofmeister effect [12]. This behavior is dominated by anions, and the Hofmeister effect of cations is not as pronounced as that of anions. For a given cation, the precipitation ability of different anions to protein is ordered as: $CO_3^{2-} > SO_4^{2-} > S_2O_3^{2-} > H_2PO_4^{-} > F^{-} > CH_3COO^{-} > Cl^{-} > Br^{-} > NO_3^{-} > I^{-} > ClO_4^{-} > SCN^{-}$ [13]. In this anion series, the ions to the left of chloride are effective in the precipitation of proteins and referred to as kosmotropes, whereas those to the right of chloride are less effective to precipitate protein and referred to as chaotropes. It provides a qualitative ranking of the effectiveness of protein precipitation. Apart from this, the Hofmeister series was also applicable to many other protein processes as previously noted [14]. In kosmotropic ions the exposure of protein surface to water is reduced to favor processes of protein folding, precipitation, aggregation, while in chaotropic ions the exposure of protein surface to water is enhanced to favor processes of protein unfolding and dissolving. The molecular mechanism for this Hofmeister effect is attributed to the direct interactions of the anions with the macromolecule and its immediately adjacent hydration shell [13,15]. Therefore, the Hofmeister effect seems to be a simple way to enhance the mechanical strength of hydrogels. Generally, kosmotropes are small and strongly hydrated to stabilize folded proteins while chaotropes are large and weakly hydrated to promote protein denaturation [16]. By applying Hofmeister effect of kosmotropic ions into natural hydrogels, ductile and strong mechanical properties are promising to achieve without sacrificing the intrinsic cellular interaction of proteins.

The natural polymer hydrogels based on Schiff base reaction can be fabricated by spontaneous crosslinking of an aldehyde group and an amino group at room temperature [17,18]. Recent researches have shown that these hydrogels have good biocompatibility and a simple preparation process while maintaining an interconnected macroporous structure and high water content [19]. Our previous studies have shown that natural polymer hydrogels based on Schiff base reaction possess effective hemostatic ability and tissue adhesion, which is a promising therapeutic strategy for wound healing [20,21]. In order to further broaden the application of these natural polymer hydrogels, it is necessary to improve their mechanical strength. The Schiff base reaction is mild and fast, and the Hofmeister effect does not require specific equipment or other complicated chemical reagents. Thus, the preparation of Hofmeister effect-enhanced natural polymer hydrogels based on Schiff base reaction is simple and easy to operate, and mechanical strength can be regulated by adjusting the type and concentration of ions.

Herein, a natural polymer hydrogel was fabricated by incorporating both chemical crosslinks and physical crosslinks, in which Hofmeister effect was combined with Schiff base reaction in synergy to enhance the mechanical strength. Gelatin is hydrolyzed from collagen that is the major component of extracellular matrix (ECM) in the native skin. Compared with collagen, gelatin does not elicit any noticeable antigenicity *in vivo*. The abundant amino groups of gelatin also allow facile modifications with other biomaterials including physical and chemical crosslinking. Based on the low antigenicity, accessible functional groups and its chemical similarities to skin ECM, gelatin was chosen as a material to fabricate hydrogel for wound healing. Then oxidized dextran (O-Dex) was prepared by oxidizing dextran with sodium periodate to get aldehyde groups. The chemical crosslinking sites were produced from amino groups of gelatin (Gel) and aldehyde groups of O-Dex through Schiff base reaction. The physical crosslinking domains were induced by kosmotropic ions through Hofmeister effect. Various kosmotropic ions were introduced to evaluate the Hofmeister effect of different ion types on the mechanical properties of Gel/O-Dex hydrogels. At the same time, the adverse effect of ions on the biocompatibility of hydrogels was also considered to choose the optimal kosmotropic ions. Following these procedures, both improved biocompatibility and mechanical behavior were ob-

tained in this study. Especially for the mechanical properties, double crosslinked networks allowed for cyclic loading and unloading to resist fatigue. The Schiff base crosslinking bonds dispersed the stress throughout the entire networks to maintain the shape of the hydrogel. When the hydrogel was deformed under stress, the physical crosslinks absorbed and dissipated energy through reversible dissociation. When the stress was removed, the physical crosslinks were formed again. Then the hydrogel returned to its original state. Moreover, Hofmeister effect only affected the physical structure of Gel/O-Dex hydrogels, and the chemical structure did not change. As a result, aldehyde groups were embedded in the center of entangled polymer chains to obtain better biocompatibility after Hofmeister effect induced the change of physical structure. Thus, we further evaluated the efficacy of Hofmeister effect-enhanced Gel/O-Dex hydrogels in the process of wound healing to verify the feasibility of Hofmeister effect to improve biocompatibility and mechanical behavior for future clinic applications.

2. Materials and methods

2.1. Chemicals and reagents

Dextran (Dex, Mw≈70000) and phosphate buffer saline (PBS, pH=7.4) were purchased from Sigma-Aldrich. Gelatin (Gel, from fish skin) was obtained from Shanghai Haiqing Water Producer Technology Co., Ltd. Sodium periodate ($NaIO_4$), ethylene glycol, anhydrous sodium carbonate (Na_2CO_3), anhydrous sodium sulfate (Na_2SO_4), sodium thiosulfate pentahydrate ($Na_2S_2O_3{\cdot}5H_2O$), and sodium dihydrogen phosphate dihydrate ($NaH_2PO_4{\cdot}2H_2O$) were obtained from Sinopharm Chemical Reagent Co., Ltd. ATDC5 cells were supplied by the institute of Biochemistry and Cell biology (Chinese Academy of Sciences, China). Cell Counting Kit-8 (CCK-8), Fetal bovine serum (FBS), DME/F12 medium and other related reagents were obtained from Gibco Life Technologies.

2.2. Synthesis of O-Dex

O-Dex was synthesized by oxidizing hydroxyl groups of dextran to aldehyde groups using sodium periodate. Firstly, dextran was dissolved in deionized water to obtain a homogeneous solution at concentration of 10% (w/v). 10% (w/v) sodium periodate solution was added dropwise to dextran solution at varying molar ratio of sodium periodate to dextran (n($NaIO_4$)/n(Dex): 0.5, 0.75, 1.0, 1.5 and 2.0). The reaction proceeded in the dark at 25°C for 4 h. Thereafter, 2 ml of ethylene glycol was added dropwise to stop the reaction. Then, the solution obtained above was purified via dialysis (Mw = 3500) against deionized water for least 3 days to remove residual sodium periodate and other small molecules. Finally, O-Dex with different percent of aldehyde groups was obtained by freezing the solution and lyophilizing in a low temperature freeze dryer.

2.3. Preparation of Hofmeister effect-enhanced Gel/O-Dex hydrogels

Firstly, O-Dex and Gel were dissolved in deionized water to prepare a homogeneous solution at concentration of 10% and 20%(w/v). 10% O-Dex and 20 % Gel solutions were mixed uniformly to allow Schiff base reaction to get Gel/O-Dex hydrogels. Hofmeister effect-enhanced Gel/O-Dex hydrogels were obtained by immersing Gel/O-Dex hydrogels in different types of Hofmeister series salt solutions for 12 h. To compare the influence of Hofmeister series on the properties of hydrogels, the molar concentration of CO_3^{2-}, SO_4^{2-}, $S_2O_3^{2-}$, and $H_2PO_4^-$ was fixed at 2 mol/L. After selecting the optimal kosmotropic ion, Gel/O-Dex hydrogels were soaked in different concentration of 10, 20, 30 wt% to explore the influence of ion concentration on the performance of Gel/O-Dex hydrogels.

2.4. Characterization of hydrogels before and after chemical or physical treatment

All hydrogels were characterized including natural gelatin, Gel/O-Dex hydrogels and Hofmeister effect-enhanced Gel/O-Dex hydrogels by various anions to compare the performance before and after chemical crosslinking of Schiff base or physical crosslinking of Hofmeister effect treatment. After immersing in kosmotrope solutions for Hofmeister effect, hydrogels were rinsed in deionized water three times (5 min each) to remove the excessive salt. The morphology, chemical structure and specific surface area of the hydrogels were evaluated by using scanning electron microscopy (SEM, JSM-5600, JEOL, Japan), Fourier transform infrared spectroscopy (FTIR, FTIR-7600, Australia), and X-ray photoelectron spectroscopy (XPS, Escalab 250Xi). Brunauer-Emmet-Teller (BET) specific surface area of hydrogels was examined after cooling in liquid nitrogen by a surface area analyser (TriStar II 3020, Micromeritics, USA). The pore size was measured by using image analysis software (Image-J, National Institutes of Health, USA) to calculate 100 pores randomly observed on the SEM images. The distribution was analyzed and plotted by using OriginPro 9.1 software (OriginLab,USA).

2.5. Mechanical evaluation of Hofmeister effect-enhanced Gel/O-Dex hydrogels

The mechanical evaluation was conducted by a universal material testing machine (Dejie, DXLL-20000, China). For the compression tests, a cylindrical hydrogel of 10 mm in diameter and height was placed on the lower plate, and the upper plate was compressed downward at a speed of 5 mm min^{-1}. For the tensile tests, the hydrogels were made into cuboid shapes (length, width and thickness of 50, 8 and 5 mm), and the effective stretching distance between the upper and lower jigs was 30 mm with a strain rate of 50 mm min^{-1}. The tensile and compression loading-unloading tests were performed at a speed of 5 mm min^{-1} for five cycles. All samples were analyzed in triplicate to assess their mechanical properties.

2.6. Swelling assessment and in vitro degradation

All hydrogels were tested in triplicate to measure swelling and degradation properties. The swelling behavior was expressed as the swelling ratio (SR). Firstly, the hydrogel samples were immersed in PBS solution for 24 h to reach equilibrium swelling state and then were wiped off to remove excess water. The swollen hydrogels were weighed as W_s. After that, the samples were lyophilized and the dry weight of the hydrogels were referred to as W_d. SR was calculated by the following equation:

$$SR = \frac{W_s - W_d}{W_d} \times 100\%$$

In vitro degradation experiments were performed in PBS buffer solution. Briefly, the hydrogels were placed in a 50 ml centrifuge tube containing 30ml of PBS solution, and then placed in a shaker at 37°C for degradation experiments. The samples were taken out at a predetermined time and the weight of degraded hydrogels were referred to as W_i after wiping off the moisture on the surface. Weight remaining (%) of hydrogels after degradation was calculated by the following formula:

$$Weight\ remaining = \frac{W_i}{W_o} \times 100\%$$

W_o was the weight of original hydrogels.

2.7. Cytotoxicity assay in vitro by CCK-8

The cytotoxicity assay was evaluated by coculturing with ATDC5 cells *in vitro* for 1, 3 and 5 days. ATDC5 cells were cultured in DME/F12 medium containing 20% fetal bovine serum and 1% penicillin/streptomycin at 5% CO_2 and 37°C. The complete medium was replaced every three days. Before ATDC5 cells seeding on the surface of hydrogels, complete medium was added to completely immerse the hydrogels overnight to full swelling. Subsequently, the medium was replaced and 100 μL of cell suspension of 1×10^5 cells/mL was added on the surface of hydrogels. The complete medium was changed every day. The cytotoxicity of hydrogels at 1, 3 and 5 days was determined by CCK-8 assay. Firstly, the culture medium was replaced with 100 μl of 10% CCK-8 solution and 300μl fresh complete medium. Then they were incubated for 1 h under light shielding conditions in a 5% CO_2 incubator at 37°C. Hereafter, 100 μl of the sample solution was transferred in a 96-well tissue culture plate to be tested. The optical density (OD) value of absorbance was measured at a wavelength of 450 nm by using a multidetection microplate reader (Multiscan GO, Thermo Scientific). The samples were tested in triplicate and the results reflected the cytotoxicity of hydrogels.

2.8. Biocompatibility measurement in vivo

The *in vivo* biocompatibility measurement was performed by implanting Gel/O-Dex hydrogels and Hofmeister effect-enhanced Gel/O-Dex hydrogels by $H_2PO_4^-$ ions into the back of SD rats. Hofmeister effect-enhanced Gel/O-Dex hydrogels were prepared by immersing in NaH_2PO_4 solution at the concentration of 20% for 12 h and subsequently rinsed in deionized water three times (5 min each) to remove the excessive salt. After the rats were anesthetized with 10% chloral hydrate (350 mg/kg), the hydrogels were implanted subcutaneously through a midline incision on the back. After 3 and 6 weeks, SD rats were sacrificed by excessive anesthesia and subcutaneous samples were collected to assess local biocompatibility *in vivo*. Local foreign-body reaction was compared between Gel/O-Dex samples and Hofmeister effect-enhanced samples. Then tissues of spleen, heart, kidney, lung and liver were collected to evaluate the function of vital organs to further confirm the biocompatibility of hydrogels *in vivo*. Vital organ tissues of normal SD rats served as control group. All tissue samples were fixed and embedded in paraffin. Then they were cut into a thickness of 8.0 μm and stained with hematoxylin-eosin (HE) for histological observation. All animal experiments were performed according to the guidelines approved by the Animal Committee of Tongji University, China.

2.9. Wound healing measurement in SD rats of full-thickness skin defects

Forty-five adult male SD rats (weighing 300 g-350 g) were performed with full-thickness skin defects for wound healing measurement. These rats were divided into three groups: control group, Gel/O-Dex hydrogel group (hydrogel group), and $H_2PO_4^-$ Hofmeister effect-enhanced Gel/O-Dex hydrogel group (Hofmeister group). After intraperitoneal injection of 10% chloral hydrate, SD rats were anesthetized and a full-thickness skin defect with the diameter of 1.5 cm was made on the dorsum of each rat with surgical scissors. The skin defects in the control group were not treated with any materials. The skin defects in the hydrogel group were treated with Gel/O-Dex hydrogels, and the skin defects in the Hofmeister group were treated with $H_2PO_4^-$ Hofmeister effect-enhanced Gel/O-Dex hydrogels. The wound morphology and healing process were observed immediately after operation, 1, 2, and 3 weeks after treatment.

2.10. Wound healing analysis and histological analysis

In the process of wound healing, the differences of wound healing among three groups were evaluated by calculating wound closure percentage. At 1, 2, and 3 weeks after treatment, all wounds were captured by high-resolution images under the backdrop of a metric ruler. The wound area was identified by the boundary of epithelialization and analyzed using Image J software. Wound closure percentage was calculated as follows: wound closure percentage (%) = (A-B/A) × 100%. Among them, A was the immediate wound area postoperatively, and B was the wound area at 1, 2, and 3 weeks after treatment.

At 1, 2, and 3 weeks after the operation, the rats were sacrificed to collect the wound and surrounding regenerated skin tissue for histological analysis. The tissue samples were fixed in 4% paraformaldehyde overnight, and then dehydrated in a series of graded ethanol. After vitrification by dimethylbenzene, the samples were incubated in paraffin-dimethylbenzene overnight to remove the dimethylbenzene and deposited in paraffin. Then the samples were cut into a thickness of 8.0 μm and adhered to a glass slide. After deparaffinization and hydration, the sections were stained with HE and Masson's trichrome staining for histological analysis.

2.11. Statistical analysis

All experiments were performed on three replicates, unless otherwise mentioned. IBM SPSS Statistics 19.0 and GraphPad Prism 5.0 software were used to perform statistical analysis. The data were presented as the mean ± standard deviation (SD). Statistical significance was considered at $p < 0.05$ via the Student's t-test. (* represented $p<0.05$.)

3. Results and discussion

3.1. Mechanism and preparation of Hofmeister effect-enhanced Gel/O-Dex hydrogels

Hofmeister effect-enhanced Gel/O-Dex hydrogels are innovative hydrogels by combining chemical crosslinking of Schiff base and physical crosslinking of Hofmeister effect based on natural gelatin hydrogels. The typical fabrication procedures are schematically depicted in Fig. 1. First, dextran was oxidized by sodium periodate to obtain aldehyde groups. Through optimizing the reaction conditions of $NaIO_4$ oxidation and the molar ratio of $NaIO_4$ to dextran n($NaIO_4$)/n(Dex), O-Dex containing different percent of aldehyde groups were obtained following dialyzed purification and freeze-dried treatment. Gelatin naturally has amino groups that allow chemical crosslinking of Schiff base by introducing aldehyde groups of O-Dex. Gelatin and O-Dex were dissolved into homogeneous solutions and uniformly mixed together. The Schiff base reaction was carried out by spontaneous crosslinking of amino groups and aldehyde groups to form Gel/O-Dex hydrogels. In the next step, Gel/O-Dex hydrogels were immersed into kosmotrope solutions and converted into Hofmeister effect-enhanced Gel/O-Dex hydrogels. Normally, the addition of kosmotropic ions into gelatin solution results in gelatin precipitation. Unlike it, when crosslinked Gel/O-Dex hydrogels are immersed into kosmotrope solutions, the crosslinking sites of Schiff base (-CH=N-) and helical bundling of gelatin chains can limit the movement of gelatin molecular chains to inhibit the process of precipitation. In this study, kosmotropic ions of Hofmeister series included CO_3^{2-}, SO_4^{2-}, $S_2O_3^{2-}$, and $H_2PO_4^-$. Through selecting the optimal kosmotropic ion, the target samples with superior mechanical properties were subsequently produced for advanced applications.

By changing the reaction conditions different percent of aldehyde groups was achieved in O-Dex. Dextran is a com-

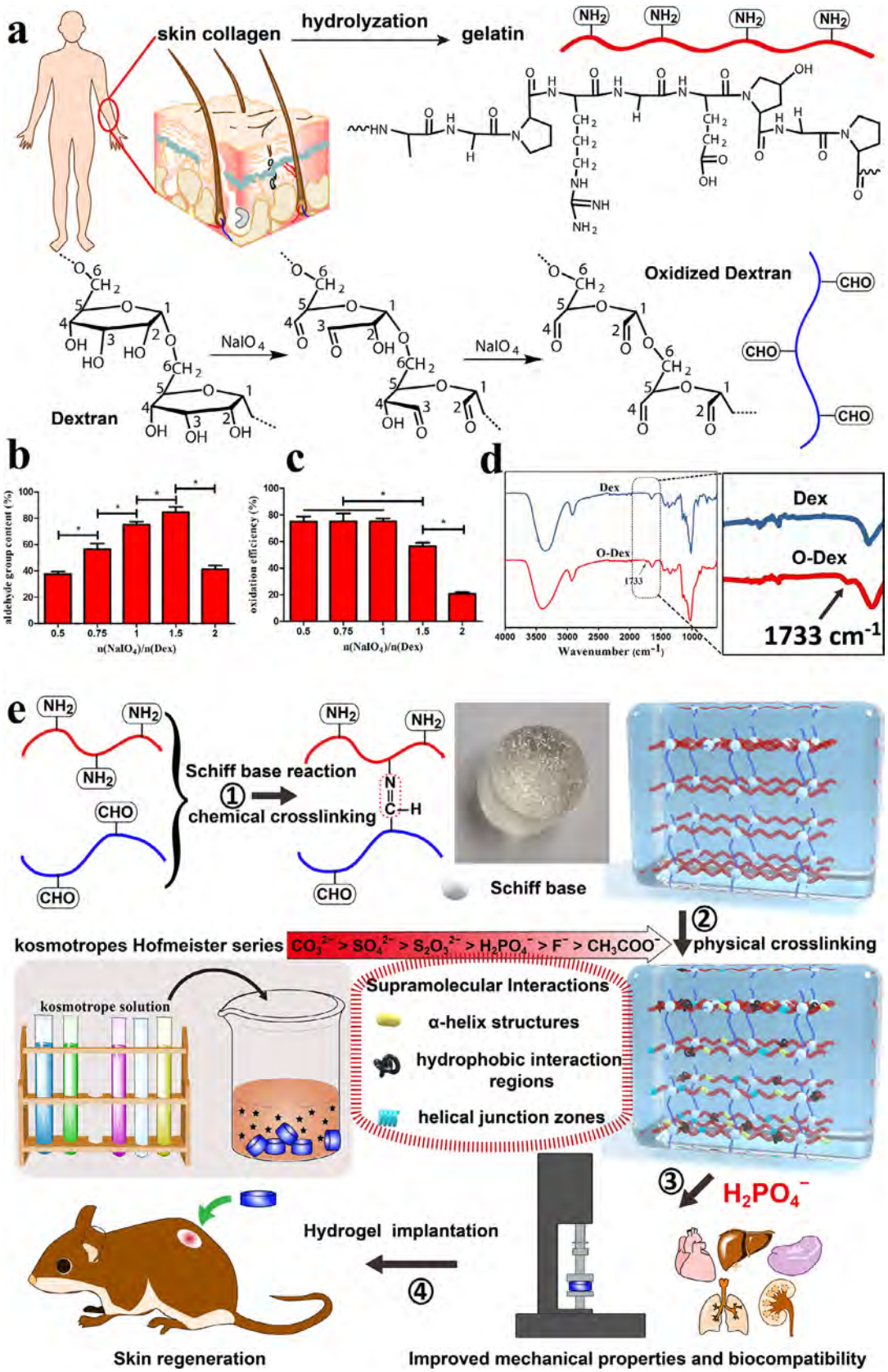

Fig. 1. (a) Gelatin is the hydrolyzed form of collagen, the major component of natural skin, wherein the abundant amino groups allow for physical and chemical crosslinking. Dextran was oxidized by sodium periodate to obtain aldehyde groups. (b) The relationship between aldehyde group content and oxidant dosage. (c) The relationship between oxidation efficiency and oxidant dosage. (d) FTIR spectra of dextran (Dex) and oxidized dextran (O-Dex). (e) Schematic diagram of preparing Hofmeister effect-enhanced Gel/O-Dex hydrogels for accelerating wound healing. Step 1: Gel/O-Dex hydrogels were prepared by chemical crosslinking of natural gelatin with aldehyde groups of O-Dex through Schiff base reaction. Step 2: Hofmeister effect-enhanced Gel/O-Dex hydrogels were prepared by inducing hydrophobic interactions among gelatin chains to form physical crosslinking of Hofmeister effect in kosmotrope solutions. Step 3 and Step 4: Considering biological essentiality and biosafety, Hofmeister effect-enhanced Gel/O-Dex hydrogels by $H_2PO_4^-$ ions were selected with improved mechanical properties and biocompatibility to promote wound healing.

plex branched polysaccharide formed by condensation of α-D-glucopyranose rings, which have glycosidic bonds predominantly linking the carbon atoms of C1 to C6. Given the specificity of periodate ions for vicinal diols, there are two sites (C2-C3 and C3-C4) that can be cleaved by periodate oxidation. The adjacent hydroxyl groups at C2-C3 or C3-C4 positions were oxidized to form aldehyde groups (Fig. 1a). If sodium periodate is excessive, it will be further oxidized to C2 and C4 positions (Fig. 1a). The amount of yielded aldehyde groups was associated with the amount of sodium periodate. Since $NaIO_4$ also has an oxidizing effect on the molecular chain and other structures of dextran, the efficiency cannot reach 100%, which is compromised by oxidative cleavage of the molecular chain and the further oxidation of aldehyde groups by $NaIO_4$.

Fig. 1b showed the relationship between aldehyde group content and oxidant dosage after full oxidation reaction. The molar ratio of sodium periodate to dextran ($n(NaIO_4)/n(Dex)$) was assigned at 0.5, 0.75, 1.0, 1.5 and 2.0. First, the percent of aldehyde groups increased rapidly with the increase of oxidant dosage (0.5 to 1.5). When the molar ratio of $NaIO_4$ to Dex was 1.50, the degree of oxidation reached the maximum of 84.64±4.08%. Thereafter, with the sodium periodate increased (1.5 to 2.0), the percent of aldehyde groups decreased to some extent. This was ascribed to the further oxidation of aldehyde groups into carboxyl groups by $NaIO_4$.

Theoretically, the mole of consumed $NaIO_4$ during the process of oxidation reaction is equivalent to the mole of cleaved glucopyranose rings. Due to the existence of other sites that can be oxidized by sodium periodate, the actual consumption of $NaIO_4$ was more than the theoretical amount, resulting in the oxidation efficiency lower than 100%. When the molar ratio of $n(NaIO_4)/n(Dex)$ was 0.5, 0.75, 1.0, 1.5 and 2.0, the oxidation efficiency was 75.00±3.82%, 75.20±5.91%, 75.11±2.26%, 56.43±2.72% and 20.71±1.28%, respectively (Fig. 1c). While the amount of $NaIO_4$ was less than the amount of Dex ($n(NaIO_4)/n(Dex)$ less than 1.0), the oxidation efficiency remained constant and approximately at 75%, indicating that 25% of consumed $NaIO_4$ reacted with other structures of dextran. While the amount of $NaIO_4$ increased and surpassed the amount of Dex ($n(NaIO_4)/n(Dex)$ more than 1.0), the oxidation efficiency decreased drastically, but the aldehyde content continued to reach the maximum of 84.64±4.08% at molar ratio of 1.50. Therefore, the oxidation efficiency and the yielded aldehyde group content cannot be optimized at the same time. In this study, we selected the molar ratio of 1.5 to yield O-Dex with the highest aldehyde group content that aimed at highest Schiff base crosslinking.

After periodate oxidation FTIR spectrum was used to confirm the introduction of aldehyde groups. As shown in Fig. 1d, the broad band of 3800-3000 cm^{-1} in the infrared absorption spectra of dextran and O-Dex was associated with the stretching vibration of hydrogen bond, indicating that both of them have high hydroxyl group content. As a strong polar group, hydroxyl group can form hydrogen bond. Due to the presence of hydroxyl groups, the hydrogen bonding occurred and the stretching vibration peak increased. It was seen from FTIR spectrum that the intensity of absorption peak of O-Dex at 3800-3000 cm^{-1} was lower than that of untreated dextran. This was ascribed to the conversion of hydroxyl groups to aldehyde groups during the oxidation process, thereby reducing the peak intensity.

After the oxidation reaction, the hydroxyl content of O-Dex decreased, and hydroxyl groups were converted into aldehyde groups or carboxyl groups, of which the aldehyde groups were main products and the carboxyl groups were over-oxidized by-products. Correspondingly, an absorption peak appeared at 1733 cm^{-1} in the infrared absorption spectrum of O-Dex, which was characteristic for the aldehyde carbonyl group C=O stretching vibration. It was worth noting that the intensity of absorption peak at 1733 cm^{-1} was relatively weak. This was due to the interaction between aldehyde group and adjacent hydroxyl group on the O-Dex molecular structure to form a hemiacetal. The formation of hemiacetal weakened the absorption peak of aldehyde group and confirmed the existence of above-mentioned reaction mechanism. Therefore, the analysis of infrared absorption spectroscopy verified the structure of dextran and O-Dex, in which O-Dex was formed by the oxidation of dextran hydroxyl groups to introduce aldehyde groups.

3.2. Chemically or physically crosslinked versions of natural gelatin hydrogels

At room temperature gelatin maintained a gel state due to the intermolecular forces between amino and carboxyl groups. Among the gelatin molecule chains, hydrogen bonds were formed to link chains and create helical junction zones that led to the formation of a gelatin hydrogel. At the temperature around 40°C, the linkages between gelatin molecular chains were destabilized so that gelatin gel transformed into a solution state and presented a random coil structure in solution. After chemically crosslinking with O-Dex, Gel/O-Dex hydrogel exhibited a stable gel state whether at room or higher temperature. The chemical crosslinking of Schiff base caused the extension of Gel and O-Dex polymer chains, resulting in the expansion of hydrogel structure and the increase of pore size. As shown in Fig. 2a, Gel/O-Dex hydrogel showed larger pore size than gelatin hydrogel. This was consistent with the reported structure of other Schiff-based hydrogels in the literatures, indicating that Schiff base reaction had been successfully applied to prepare Gel/O-Dex hydrogels. Pore size, porosity, and pore structure are important factors to be considered, because they are closely associated with the supply of oxygen and nutrients to cells and the removal of metabolic waste while implanting hydrogel *in vivo*.

To further confirm the inner architectures of gelatin and Gel/O-Dex hydrogels, Brunauer-Emmet-Teller (BET) specific surface area tests of the freeze-dried samples were performed to estimate the porosity. The nitrogen adsorption/desorption isotherms of natural gelatin hydrogel and Gel/O-Dex hydrogel were shown in Fig. 2b. According to the Brunauer classification, the adsorption/desorption curve corresponded to a typical type III isotherm that did not exhibit any limiting adsorption at high relative pressures [22]. With the increase of the relative pressure, the adsorption amount increased gradually. Then the adsorption became quite abrupt when it was close to the saturation vapor pressure, indicating that the adsorption on these two kinds of macroporous solids proceeded through unrestricted multilayer formation. As also shown in Fig. 2b, the adsorption process was accompanied by adsorption-desorption hysteresis. According to the IUPAC recommendations, the hysteresis loops observed in gelatin and Gel/O-Dex hydrogels were classified as type H3 loops that did not level off at relative pressures close to the saturation vapor pressure ($P/P_0=1$) [23]. The hysteresis loops revealed the thermodynamic metastability of adsorption-desorption and the property of pore connectivity. In the processes of adsorption and desorption, capillary condensation or capillary evaporation was delayed respectively and did not take place at the same pressure that the gaslike and liquidlike phases coexisted in the pores. The pore connectivity demonstrated by hysteresis loops was consistent with the inner architectures of gelatin and Gel/O-Dex hydrogels observed by scanning electron microscope. The network of pore connectivity was expected to play an important role in adsorption-desorption processes. Because larger pores were connected to the surrounding smaller pores, at the relative pressure corresponding to the capillary evaporation of larger pores, the smaller pores were still filled with the condensed adsorbate and the larger pores were not emptied completely. Only at the relative pressure corresponding to the capillary evaporation of smaller connecting pores, larger pores were emptied. Thus, type

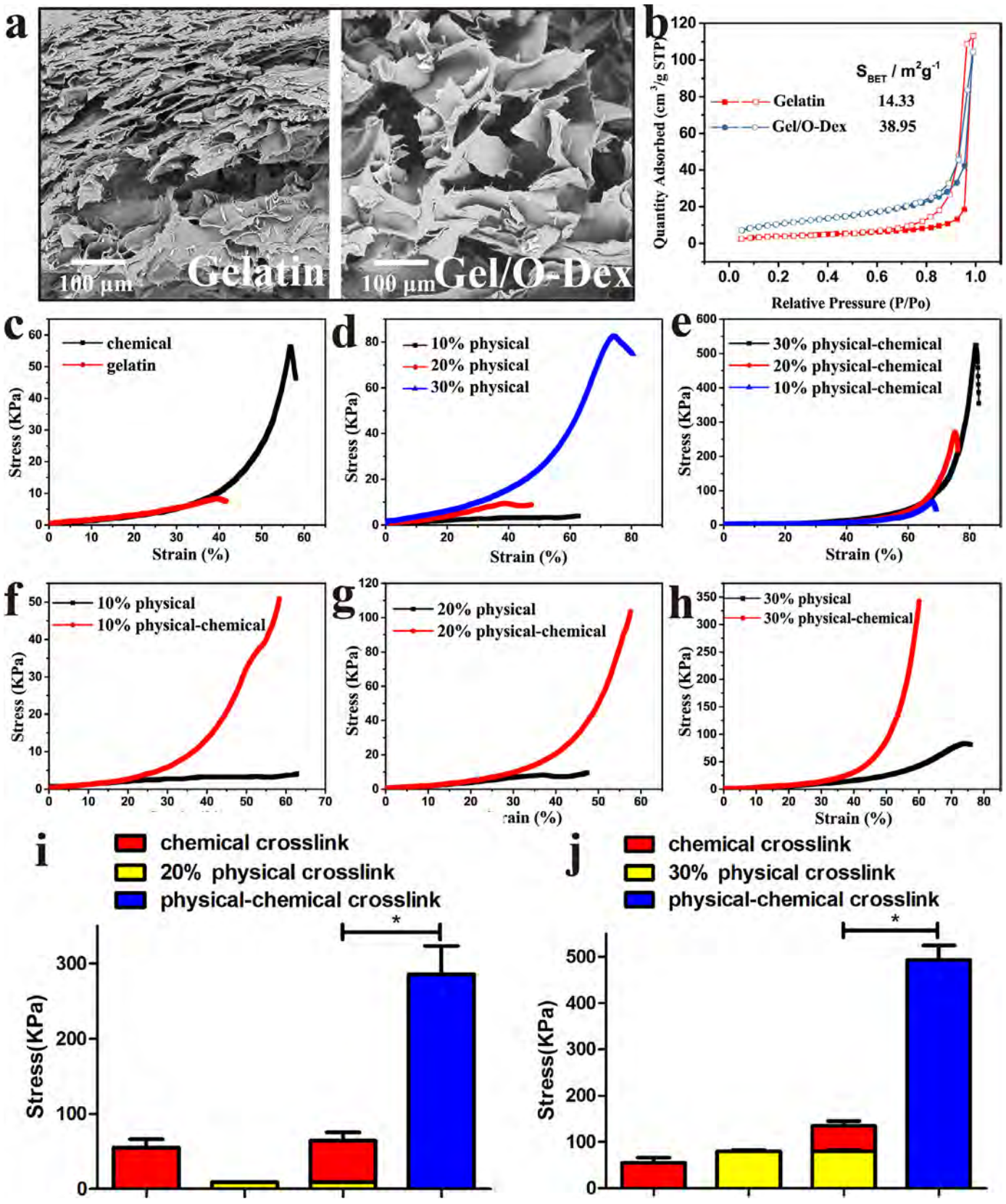

Fig. 2. The method of crosslinking (Schiff base and Hofmeister effect) was shown to play an important role in the inner architecture and mechanical strength of natural gelatin hydrogels. (a) SEM images of natural gelatin hydrogel and Gel/O-Dex hydrogel after chemical crosslinking of Schiff base. (b) Typical nitrogen adsorption-desorption isotherms of gelatin and Gel/O-Dex hydrogels. (c–e) The influence of chemical crosslinking, physical crosslinking and their combination on the mechanical properties of hydrogels. (chemical: Schiff-based chemical crosslinking; 10%, 20%, 30% physical: $H_2PO_4^-$ physical crosslinking at the concentration of 10%, 20%, 30%; physical-chemical: the combination of chemical and physical crosslinking.) (f–h) Based on chemical crosslinking, physical crosslinking significantly enhanced the mechanical properties of hydrogels at the scale of several times. (i, j) The mechanical properties enhanced by the synergistic effect of physical-chemical crosslinking were significantly higher than the adding up of single physical with single chemical crosslinking.

H3 hysteresis loops showed the non-uniformity of the pores. Correspondingly, the BET specific surface areas of gelatin and Gel/O-Dex hydrogels were 14.33 and 38.95 $m^2\ g^{-1}$, respectively. Compared with gelatin hydrogel, the specific surface area of Gel/O-Dex hydrogel was increased by 171.8%, which was mainly due to the extension of polymer chains after chemical crosslinking of Schiff base.

In addition to the inner architecture, the method of crosslinking also played varying effect on the mechanical strength of hydrogels. Compared with natural gelatin hydrogel, chemical crosslinking enhanced mechanical strength of Gel/O-Dex hydrogel by more than five times (Fig. 2c). Moreover, physical crosslinking also increased the mechanical properties to varying degrees. After soaking in 10, 20, and 30% NaH_2PO_4 aqueous solutions, the physical crosslinking of Hofmeister effect was introduced in gelatin hydrogels. The compressive strength of gelatin hydrogels treated with 10 % NaH_2PO_4 was 2.77 kPa. After soaking in 20 and 30% NaH_2PO_4 solutions, the compressive strengths of gelatin hydrogels were 16.65 and 83.09 kPa, exhibiting superior mechanical properties (Fig. 2d). By combination of physical and chemical crosslinking, the mechanical properties showed varying degrees of strength variation with the similar regularity (Fig. 2e). Specifically, whether it was 10% or 20%, or even 30%, the physical crosslinking significantly improved the mechanical properties of hydrogels by several times on the basis of chemical crosslinking (Fig. 2f–h). Further analysis, we found that the increase of mechanical strength was limited by single physical crosslinking or single chemical crosslinking. By combination of them, physical and chemical crosslinking acted synergistically to improve mechanical strength exponentially rather than simply accumulate in hydrogels. The adding up of single chemical with single physical crosslinking (chemical crosslink plus 20% or 30% physical crosslink) was significantly lower than the mechanical strength of physical-chemical crosslinking (Fig. 2i, j). Thus, for natural gelatin hydrogels, the compressive strength was multiplied by two orders of magnitude after chemical crosslinking of Schiff base and reinforced mechanically by Hofmeister effect.

3.3. The effect of Hofmeister series on the properties of Gel/O-Dex hydrogels

The type and concentration of kosmotropic ions exhibited a significant role in regulating the morphology and mechanical strength of hydrogels. To systematically evaluate the influence of Hofmeister series on the properties of Gel/O-Dex hydrogels, the preformed Gel/O-Dex hydrogels were soaked in a series of kosmotrope solutions (the ions to the left of chloride including CO_3^{2-}, SO_4^{2-}, $S_2O_3^{2-}$, and $H_2PO_4^-$) and the molar concentration of ions was fixed at 2 mol/L. As shown in Fig. 3a, Gel/O-Dex hydrogels represented a transparent and clear gel phase. After treatment with various kosmotropic ions, the hydrogels underwent varying degrees of shrinkage and showed different color in appearance. The shrinkage intensity of hydrogel shapes was shown as $CO_3^{2-} > SO_4^{2-} > S_2O_3^{2-} > H_2PO_4^-$. After Hofmeister effect-enhanced Gel/O-Dex hydrogels were snap-frozen and lyophilized using liquid nitrogen, the view of their freeze-dried state was shown in Fig. 3a.

The microscopic morphology of hydrogels was a porous network structure, which was mainly due to the interpenetration of molecular chains during the crosslinking process [24–26]. After the enhancement of Hofmeister effect, pore size of the hydrogels was shown to exquisitely depend on the type of kosmotropic ions. The Hofmeister series is usually ordered as: $CO_3^{2-} > SO_4^{2-} > S_2O_3^{2-} > H_2PO_4^- > F^- > CH_3COO^- > Cl^- > Br^- > NO_3^- > I^- > ClO_4^- > SCN^-$, according to their ability to promote the precipitation of proteins [13,27]. For anion with better precipitation ability, Hofmeister effect exhibited a stronger influence to reduce the pore size of the hydrogel. The pore size of different treatment was shown in Fig. 3b. The shrinkage intensity of the apertures was consistent with the order of Hofmeister series.

As shown in Fig. 3c, the untreated Gel/O-Dex hydrogel exhibited a porous network structure and the micropores were interconnected and uniformly distributed in the hydrogel. After CO_3^{2-} treatment, the inner architecture significantly changed due to the strong precipitation of proteins and the porous structure was complete destroyed. After SO_4^{2-} treatment, the porous structure also underwent such severe shrinkage that the diameters of pore size were mostly less than 50 μm on statistical frequency distribution analysis (Fig. 3d). This was not conducive to nutrient exchange of cell ingrowth when implanted *in vivo*. For $S_2O_3^{2-}$ and $H_2PO_4^-$ anions, the porous structures of the hydrogels were well maintained although the pore size was decreased after treatment. SEM observation showed that the inner architectures were not severely damaged, which was crucial for their biological applications (Fig. 3c). And that, pore size of $H_2PO_4^-$ treated hydrogel was larger than that of $S_2O_3^{2-}$ treated hydrogel (Fig. 3d). Thus, pore size of Hofmeister effect-enhanced Gel/O-Dex hydrogels was shown to be sensitive to the order of Hofmeister series. Superior precipitated anion was preferable to shrink the inner apertures. Pore size greater than the diameter of a cell was favorable to migration of surrounding cells, whereas an impermeable scaffold or with too small pores would not provide any assistance for cell ingrowth. Compared with $S_2O_3^{2-}$ and $H_2PO_4^-$ anions, Hofmeister effect of CO_3^{2-} and SO_4^{2-} anions were not suitable to enhance natural derived hydrogels for tissue engineering application.

Similarly, the compressive and tensile strength of Gel/O-Dex hydrogels treated with different anions was also consistent with the order of Hofmeister series. As shown in Fig. 3e–h, the interactions induced by the Hofmeister effect of kosmotrope solutions endowed Gel/O-Dex hydrogels with improved mechanical properties. After treatment with CO_3^{2-} ion, hydrogel sustained the highest compressive stress, ten times of that of untreated Gel/O-Dex hydrogel. When the hydrogel was soaked in other anion solution, the ultimate compressive stress gradually decreased due to the reduced Hofmeister effect (Fig. 3f). The tensile properties enhanced by Hofmeister effect also showed similar results. CO_3^{2-} treated hydrogel possessed the tensile strength of 108.54±9.28 kPa, which was higher than other anions. The Gel/O-Dex hydrogels treated with SO_4^{2-}, $S_2O_3^{2-}$, and $H_2PO_4^-$ showed a gradual decline in tensile properties, but were significantly higher than that of untreated hydrogels (Fig. 3g, h).

Thus, as the effect of anions on protein precipitation decreased, the mechanical strength of the hydrogel decreased. This anion type to mechanical change phenomenon can be explained by the formation of additional physical crosslinking networks, which are tough and require more stress to compress and stretch. Generally, Hofmeister effect results in molecular chain folding, precipitation, aggregation, playing the significant effect on the protein. In the Gel/O-Dex hydrogels treated with anions, Hofmeister effect may theoretically cause α-helix structures, hydrophobic interactions, and helical junctions of Gel protein molecular chains. This mechanism will be discussed and verified in the following results.

3.4. The effect of $H_2PO_4^-$ ions on the properties of Hofmeister effect-enhanced Gel/O-Dex hydrogels

Except for the type, the concentration of anions also has an influence on the properties of Gel/O-Dex hydrogels. Bicarbonate-carbonic acid buffer(H_2CO_3/$NaHCO_3$) and phosphate buffer (Na_2HPO_4/ NaH_2PO_4) are important buffering systems that exist in the human body to prevent a radical change in fluid pH by absorbing excess hydrogen or hydroxyl ions, so that the pH of the blood and other fluids are maintained within a certain range (pH between 7.35 and 7.45). They regulate not only acid-base balance

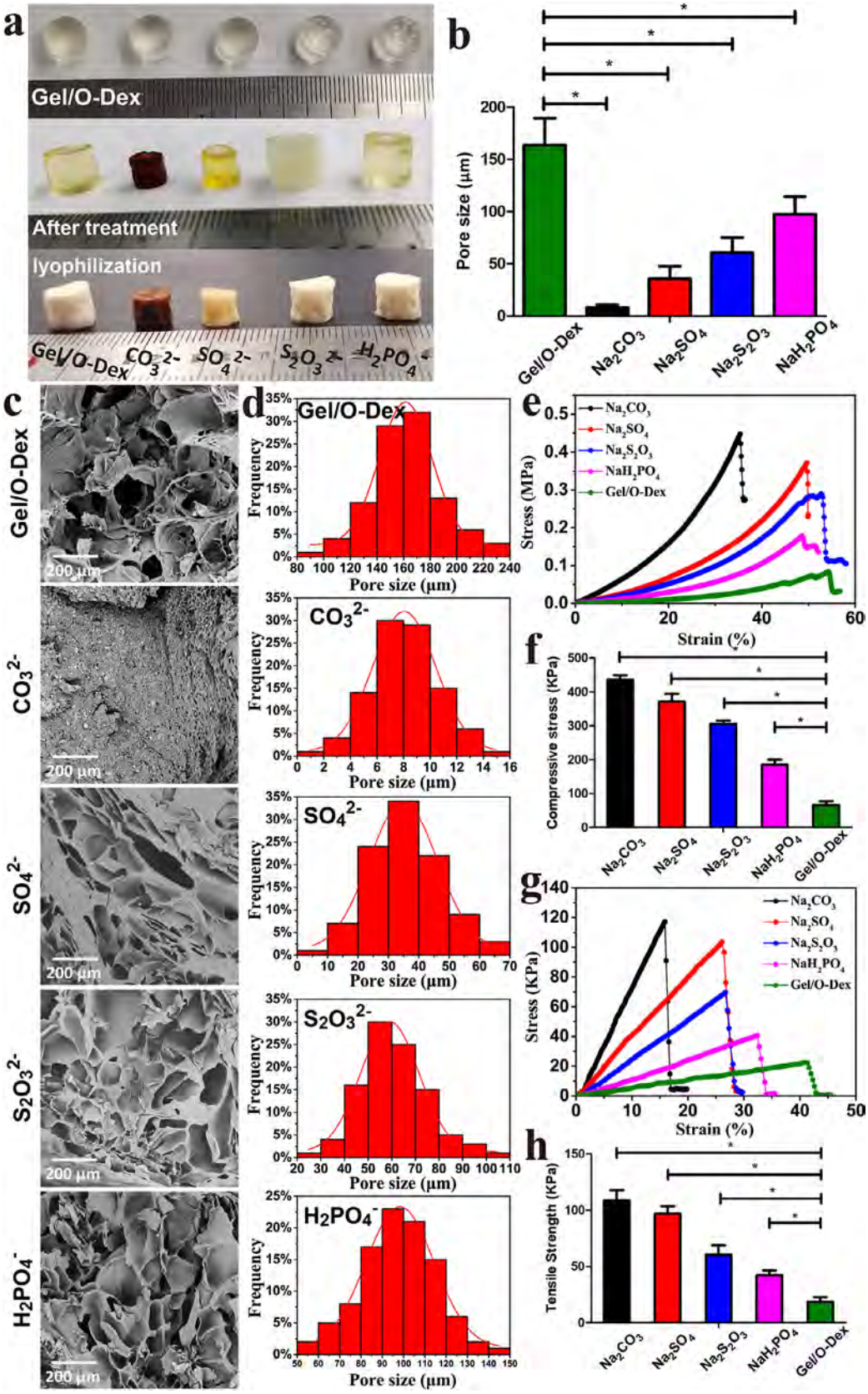

Fig. 3. Gel/O-Dex hydrogels treated with different anions in the Hofmeister series. (a) General images of Gel/O-Dex hydrogels before and after treatment with different anions (CO_3^{2-}, SO_4^{2-}, $S_2O_3^{2-}$, $H_2PO_4^-$ at the concentration of 2 mol/L) and view of their freeze-dried state. (b) Comparison of pore size for Gel/O-Dex hydrogels treated with different solutions. (c, d) SEM images and pore size distribution of Gel/O-Dex hydrogels before and after treatment with CO_3^{2-}, SO_4^{2-}, $S_2O_3^{2-}$, $H_2PO_4^-$. (e, f) Compressive stress-strain curves and strength of Gel/O-Dex hydrogels treated with different anions. (g, h) Tensile stress-strain curves and strength of Gel/O-Dex hydrogels treated with different anions.

and osmotic pressure, but also maintain the normal physiological functions of cells [28,29]. Both CO_3^{2-} and $H_2PO_4^-$ are essential inorganic anions for life activities and cell proliferation. Considering the destructive effect of CO_3^{2-} on the porous structure of Gel/O-Dex hydrogels mentioned above and the non-biogenesis of other kosmotropic ions, we choose $H_2PO_4^-$ ions instead of CO_3^{2-} and other kosmotropic ions for further investigation and advanced applications.

After immersing in NaH_2PO_4 solutions of different concentrations, Gel/O-Dex hydrogels exhibited varying degrees of shrinkage. With the increase of NaH_2PO_4 concentration from 10% to 30%, the hydrogels underwent gradual dehydration and contraction due to the elevated osmotic pressure in the surrounding environment. At high concentration of 30%, Gel/O-Dex hydrogels became highly dehydrated and shrunken while still maintained in transparent (Fig. 4a). The corresponding lyophilized hydrogels were prepared to explore their inner architectures. As shown in Fig. 4b, the NaH_2PO_4 concentration of 10% and 20% had a pronounced effect on the interaction of Gel protein molecular chains to reduce pore size, while showed no destructive influence on the porous morphology of hydrogels. But the high concentration of 30% NaH_2PO_4 caused Gel chain precipitation and aggregation, which severely damaged the porous structure of Gel/O-Dex hydrogel. Thus, the Hofmeister effect of $H_2PO_4^-$ ions affected the inner architectures of Gel/O-Dex hydrogels. As the concentration increased, the pore size significantly decreased (Fig. 4c). When the concentration reached to 30%, the inner apertures of the hydrogels contracted severely, accompanied by the destruction of porosity.

Fig. 4d showed the equilibrium water content and swelling ratio of hydrogels. The swelling ratio of untreated Gel/O-Dex and Hofmeister effect-enhanced Gel/O-Dex hydrogels were above 400%, indicating that large amounts of water was retained in hydrogel polymeric networks. Due to this unique property, these hydrogels were more likely to resemble natural soft tissues. After being treated with NaH_2PO_4 solution, the water content was significantly reduced at the equilibrium swelling state of hydrogels. As the concentration of NaH_2PO_4 solution increased, the swelling ratio of hydrogel decreased drastically. With the enhancement of Hofmeister effect by $H_2PO_4^-$ ions, the entanglement of Gel molecular chains increased, resulting in the helical junctions and hydrophobic interactions of the polymer chains. This feature maintained the stability of hydrogel structure and significantly inhibited the swelling behavior of hydrogel in an aqueous environment.

Furthermore, similar results were observed in the degradation tests (Fig. 4e). During the entire experimental period of 28 days, all Hofmeister effect-enhanced Gel/O-Dex hydrogels degraded over time. With the increase of NaH_2PO_4 concentration from 10 to 30%, hydrogels exhibited a decreased degradation rate. The weight remaining of Gel/O-Dex hydrogel treated with 30% NaH_2PO_4 was significantly higher than that of 10% and 20% NaH_2PO_4 treated hydrogels. Reduced degradation rates contribute to longer-lasting function of hydrogels in the living organisms, which is beneficial for further biological application of Hofmeister effect-enhanced hydrogels.

To explain the above results and clarify the possible mechanism, we analyzed and confirmed the type of interactions among molecular chains. Fourier transform infrared (FTIR) spectra were performed in the Gel/O-Dex hydrogels untreated or treated by NaH_2PO_4 solution at different concentrations. As shown in Fig. 4f, the broad absorption peak at around 3410 cm^{-1} in all samples was ascribed to the O–H stretching vibrations of hydrogen bonds. The characteristic absorption peaks at 2923 cm^{-1} and 2854 cm^{-1} were corresponding to the asymmetric and symmetric stretching vibrations of CH_2 [30]. Hydrophobic interactions have been reported in the process of protein assembly that hydrophobic chains exclude water molecules from the volumes and present regions of space where hydrogen bonding cannot occur [31]. When the NaH_2PO_4 concentration increased to 30%, the intensity of hydrogen bonds at around 3410 cm^{-1} decreased drastically, indicating that hydrophobic interactions were induced among Gel molecular chains. As a result, water tended to move away from the hydrogels and the shrinkage phenomenon was observed in appearance.

In addition, the absorption peak appearing at 1635 cm^{-1} was attributed to the C=O stretching vibration (amide I band). The peak at 1538 cm^{-1} was associated with the N-H stretching vibration (amide II band). The peak at 1290 cm^{-1} was assigned to the C–N stretching vibration (amide III band). The amide III Region of FTIR spectroscopy has been developed to analyze protein secondary structure such as α-helix, β-sheet, β-turn, and random coil [32,33]. The absorption peak for α-helix is around 1300 cm^{-1} and the absorption peak for β-sheet is around 1235 cm^{-1}, while the frequency window of 1260−1280 cm^{-1} is assigned for β-turn and 1240−1260 cm^{-1} for random coil [34]. As the NaH_2PO_4 concentration increased the intensity of amide III band at 1290 cm^{-1} increased, which indicated that the intramolecular α-helix structures of Gel molecular chains were generated after treating Gel/O-Dex hydrogels with $H_2PO_4^-$ ions. Therefore, Hofmeister effect generated strong hydrophobic interaction regions and α-helix structures among Gel molecular chains to obtain enhanced mechanical properties.

Besides, the absorption peaks appearing at the positions of 1097, 935, and 541 cm^{-1} were attributed to the $H_2PO_4^-$ stretching vibration [35]. It indicated that NaH_2PO_4 was preserved in the crosslinking networks when Gel/O-Dex hydrogels were physically crosslinked through Hofmeister effect. The infrared absorption peaks of Gel/O-Dex hydrogels treated with different concentrations of $H_2PO_4^-$ ions were basically similar. Compared with untreated Gel/O-Dex hydrogels, the chemical structure of treated hydrogels did not change significantly after being soaked in NaH_2PO_4 solutions.

3.5. The mechanical properties of Hofmeister effect-enhanced Gel/O-Dex hydrogels by $H_2PO_4^-$ ions

After the hydrophobic interactions and α-helix structures among Gel molecular chains were induced by Hofmeister effect of NaH_2PO_4 solutions, Gel/O-Dex hydrogels were endowed with improved mechanical properties. As shown in Fig. 5a, Gel/O-Dex hydrogels ruptured at a small tensile strength of 28.9 kPa before treatment with NaH_2PO_4. When Gel/O-Dex hydrogels were soaked in a 10% NaH_2PO_4 solution, the ruptured tensile strength slightly decreased to 20.4 kPa due to the dominating swelling behavior in lower concentration. With the increase of NaH_2PO_4 concentration from 10% to 30%, a significant enhancement was achieved in the ultimate tensile strength at rupture. The maximum tensile strength further increased to 110.7 kPa at a 30% NaH_2PO_4 concentration, which was 383% of that (28.9 kPa) of the untreated Gel/O-Dex hydrogels.

Thereafter, compressive and tensile loading-unloading tests were performed to evaluate the mechanical behavior and energy dissipation of the hydrogels. As shown in Fig. 5b, c, for 30% NaH_2PO_4 treated Gel/O-Dex hydrogels, the loading curve differed from the unloading curve and a hysteresis loop was observed in both compressive and tensile tests. Typically, the hysteresis loop in the loading-unloading curves represented the energy dissipation of each cycle. The untreated Gel/O-Dex hydrogels displayed negligible hysteresis loop and no energy dissipation, which was due to the existence of only chemical crosslinking. After salt treatment, the area of hysteresis loop became obvious as NaH_2PO_4 concentration increased, especially for 30%. This was consistent with the gradual increase of mechanical strength at ultimate rupture. Therefore, Hofmeister effect increased the entanglement between Gel molec-

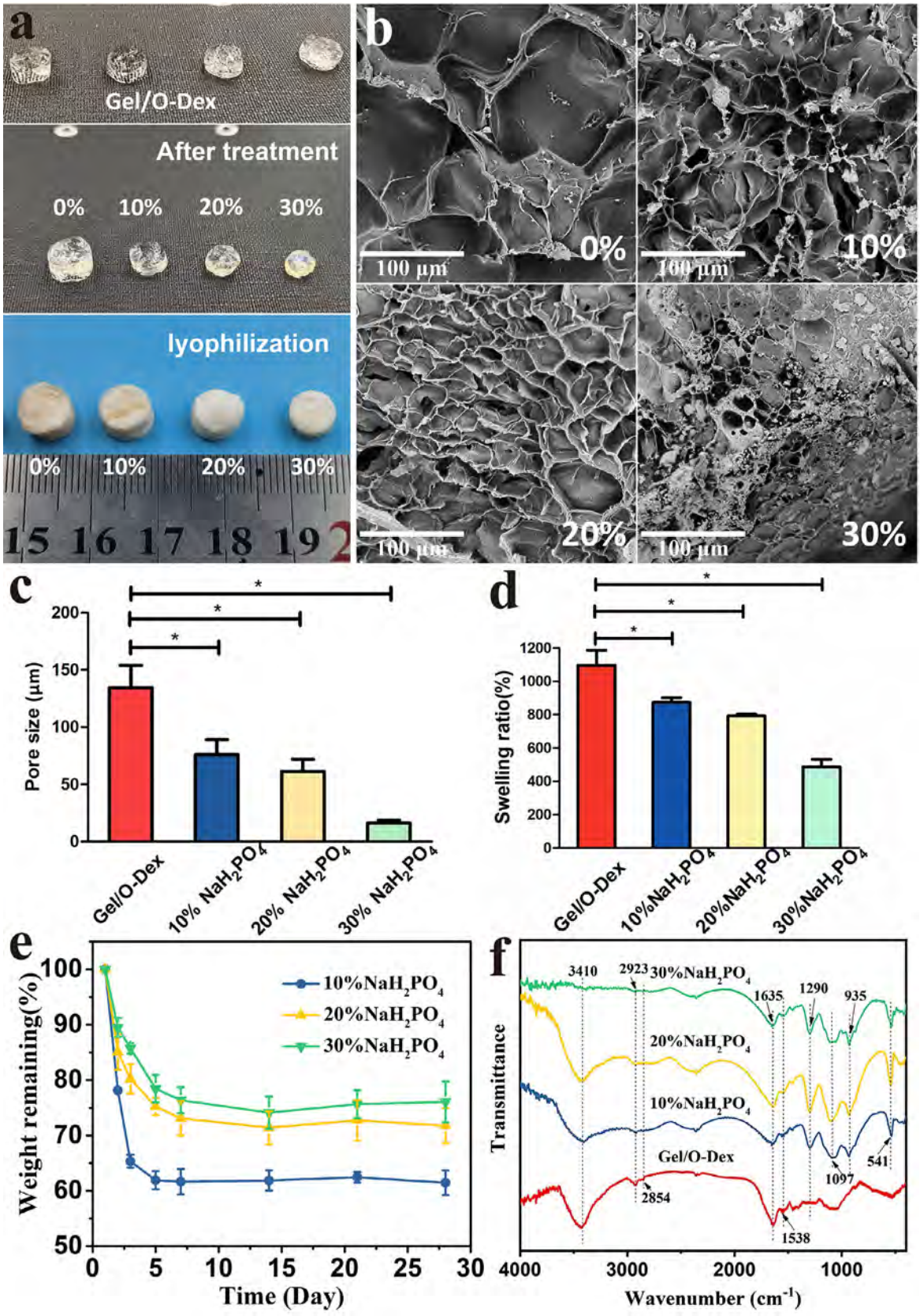

Fig. 4. Gel/O-Dex hydrogels treated with different concentration of NaH_2PO_4 solution. (a) General view of untreated or treated Gel/O-Dex hydrogels after immersion in concentration of 10%, 20%, 30% NaH_2PO_4 solution and macroscopic observation of the corresponding samples after lyophilized treatment. (b) SEM images of Gel/O-Dex hydrogels and treated with 10%, 20%, 30% NaH_2PO_4. (c) Comparison of pore size for Gel/O-Dex hydrogels treated with different concentration solution. (d–f) Swelling (d), degradation behaviors (e) and FTIR spectra (f) of Gel/O-Dex hydrogels treated with different concentration of NaH_2PO_4 solution.

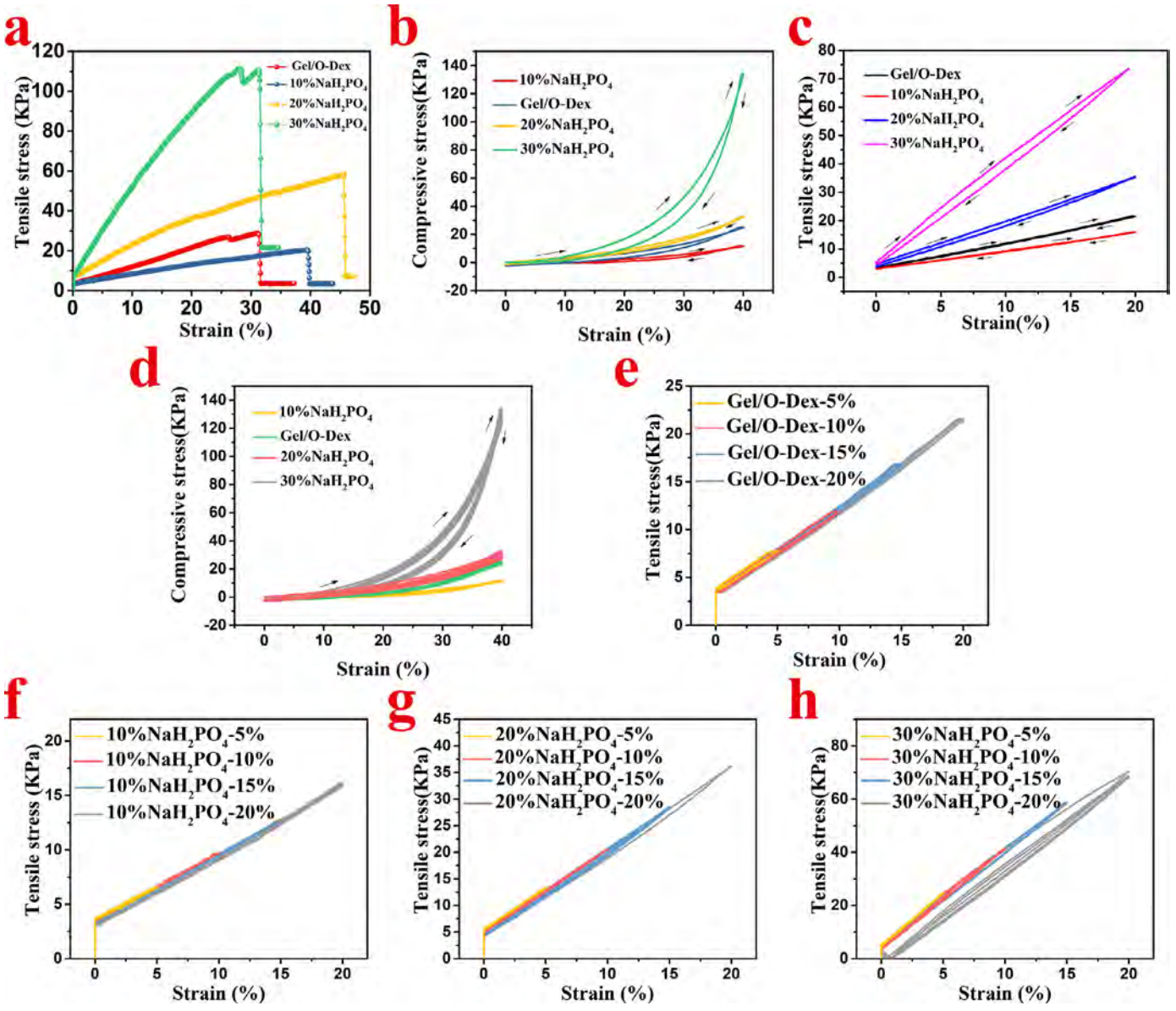

Fig. 5. Mechanical properties of Hofmeister effect-enhanced Gel/O-Dex hydrogels by $H_2PO_4^-$ ions at different concentrations: (a) tensile stress-strain curves; (b) compressive loading-unloading tests; (c) tensile loading-unloading tests; (d) five cycles of compressive loading-unloading tests; (e-h) five cycles of tensile loading-unloading tests at strain of 5%, 10%, 15%, 20%.

ular chains remarkably, resulting in a significant increase in the mechanical strength of hydrogels at rupture and allowing for obvious hysteresis loops and energy dissipation. While the external force was exerted on the hydrogels, the physical crosslinking domains by Hofmeister effect can decrosslink and dissociate to dissipate a certain amount of energy.

To further evaluate the antifatigue and shape recovery properties of $H_2PO_4^-$-enhanced Gel/O-Dex hydrogels, five cycles of loading-unloading tests were performed on hydrogels untreated or treated by NaH_2PO_4 aqueous solution at different concentrations without pausing between the cycles. Fig. 5d–h showed the loading and unloading curves at a set strain of 40% for the compression and 5%, 10%, 15%, 20% for the tension. In the five cyclic loading-unloading compressive tests, the stress and strain of all hydrogels did not change substantially in the strain range of 10-40 %, indicating that no obvious plastic deformation and strength degradation occurred after cyclic mechanical deformation. The same phenomenon was observed in the tensile tests under loading-unloading cycles with varying maximum strains. At the strain range of 5-15%, no change was detected in the stress-strain curves of five cycles. Only at the tensile strain of 20%, 30% NaH_2PO_4 treated Gel/O-Dex hydrogels behaved elastically with hysteresis loops, which was also observed in compressive tests. The shape-recovery properties and fatigue resistance of all hydrogels under loading-unloading cycles were attributed to chemical and physical crosslinks and hysteresis properties were induced by Hofmeister effect at a NaH_2PO_4 concentration of 30%.

Thus, the Hofmeister effect-enhanced hydrogels showed adjustable mechanical properties to meet the needs for different parts of human skin. Natural skin is capable to stretch and snap back to its original shape, exhibiting various deformations (elongation, compression and bending) or a repetition of their combinations. These properties demand wound dressings for skin defects to possess suitable stretchable and compressive properties, and fast shape-recovery ability to bear deformation. The resulting hydrogels possessed elasticity, improved strength, recoverability and effectively dissipated the energy from large stress to resist fatigue. These mechanical characteristics are in line with the demands of

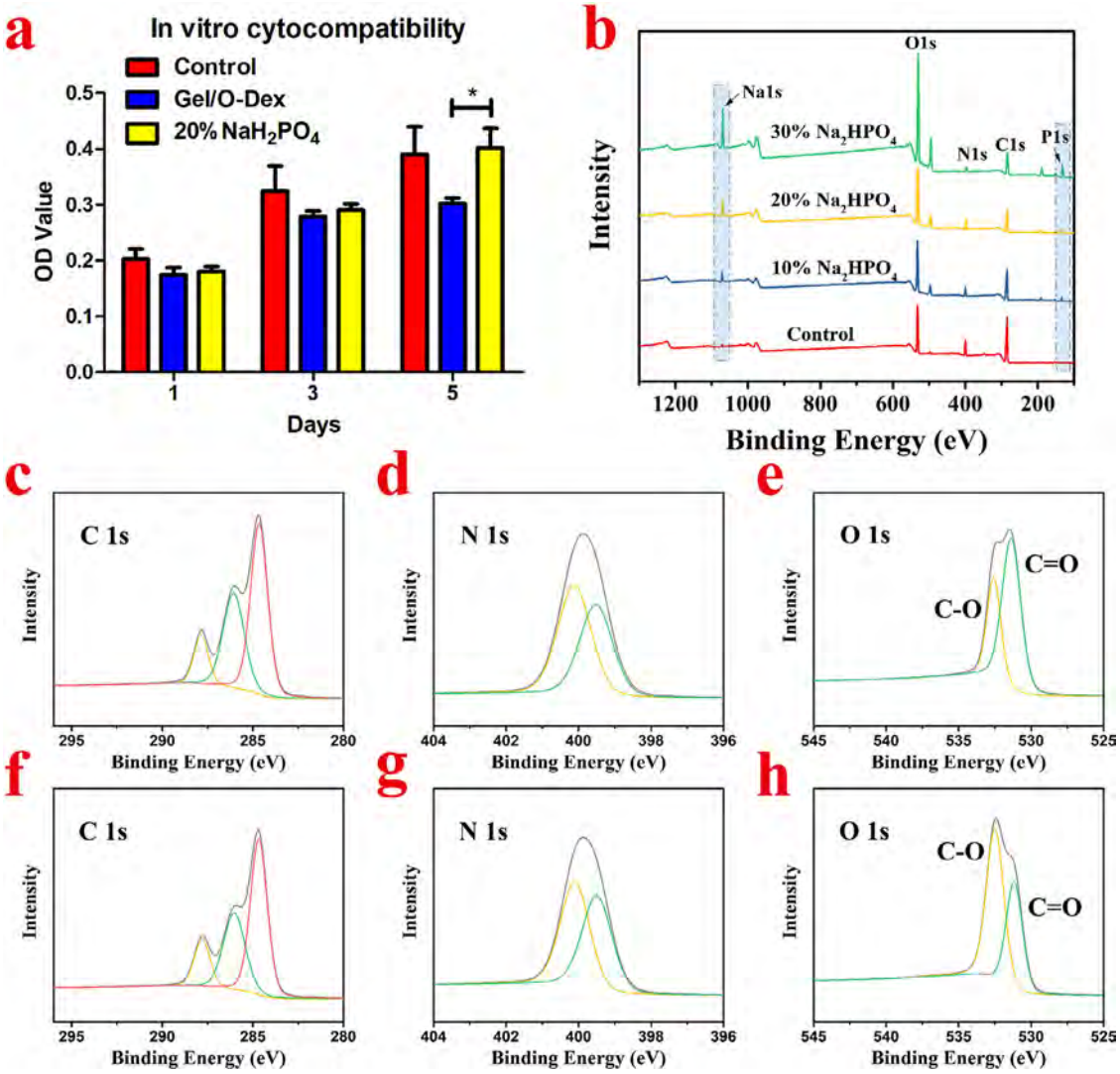

Fig. 6. (a) Cytotoxicity of Gel/O-Dex hydrogels and 20% NaH_2PO_4 treated Gel/O-Dex hydrogels by CCK-8 assay. XPS results of Gel/O-Dex hydrogels untreated and treated with different concentrations of NaH_2PO_4 solutions: (b) XPS survey spectra; (c–e) high-resolution C 1s, N 1s and O 1s XPS spectrum of the untreated Gel/O-Dex hydrogels; (f–g) high-resolution C 1s, N 1s and O 1s XPS spectrum of 20% NaH_2PO_4 treated Gel/O-Dex hydrogels.

skin substitutes and therefore have a certain prospect of medical translation.

3.6. The improved biocompatibility and its mechanism for Hofmeister effect-enhanced Gel/O-Dex hydrogels by $H_2PO_4^-$ ions

To determine if Hofmeister effect-enhanced Gel/O-Dex hydrogels are biocompatible and will function in a biologically appropriate manner in the *in vivo* environment, meaningful testing procedures were performed including *in vitro* assessment of cytotoxicity and *in vivo* assessment of tissue compatibility. *In vitro* cytotoxicity measurement focused on the potential effect of hydrogels on cell viability and proliferation. As shown in Fig. 6a, all three groups displayed a significant increase in cell viability and proliferation during the entire culture period. Among them, cell proliferation of Gel/O-Dex hydrogels was slightly lower than that of Gel/O-Dex hydrogels treated with 20% NaH_2PO_4 solution and control group, indicating that the enhancement of Hofmeister effect improved hydrogel cytocompatibility. Between Hofmeister effect-enhanced hydrogels and control group, there was no conspicuous difference in cell viability and proliferation, revealing that Hofmeister effect-enhanced Gel/O-Dex hydrogels by $H_2PO_4^-$ ions caused no toxic effects of cellular death and activity inhibition at the cellular level. As for the elevated osmotic pressure of 20% NaH_2PO_4 treatment, we rinsed Hofmeister effect-enhanced Gel/O-Dex hydrogels in deionized water to remove the excessive salt. This was consistent with previous studies [36,37], in which ion-reinforced hydrogels also supported cell adhesion and proliferation.

To further illustrate the reasons for the improved biocompatibility of hydrogels after $H_2PO_4^-$ ions treatment, XPS was performed to analyze the elemental composition and chemical bonds of the surface of the hydrogels. The XPS survey spectra were shown in Fig. 6b. The emission peaks at 531.79, 399.84, and 297.98 eV for all four groups corresponded respectively to O 1s, N 1s and C 1s, mainly originating from gelatin and oxidized dextran in the hydrogels [38,39]. In comparison with the untreated Gel/O-Dex hydrogels, two new characteristic peaks emerged at 1071.13 eV and 132.97 eV for all NaH_2PO_4 treated groups. They corresponded to Na 1s and P 1s, mainly deriving from NaH_2PO_4. Compared with 10% and 20% NaH_2PO_4 treatment groups, 30% NaH_2PO_4 treatment group showed higher emission peaks of Na 1s and P 1s. More specifically, as the concentration of NaH_2PO_4 increased from 10 to 30%, the atomic percentage of Na and P increased respectively from 2.39 to 6.82% and 3.76 to 7.98% (Table 1). Then the change of chemical bonds was also analyzed from high-resolution XPS spectra. As shown in Fig. 6c–h, there

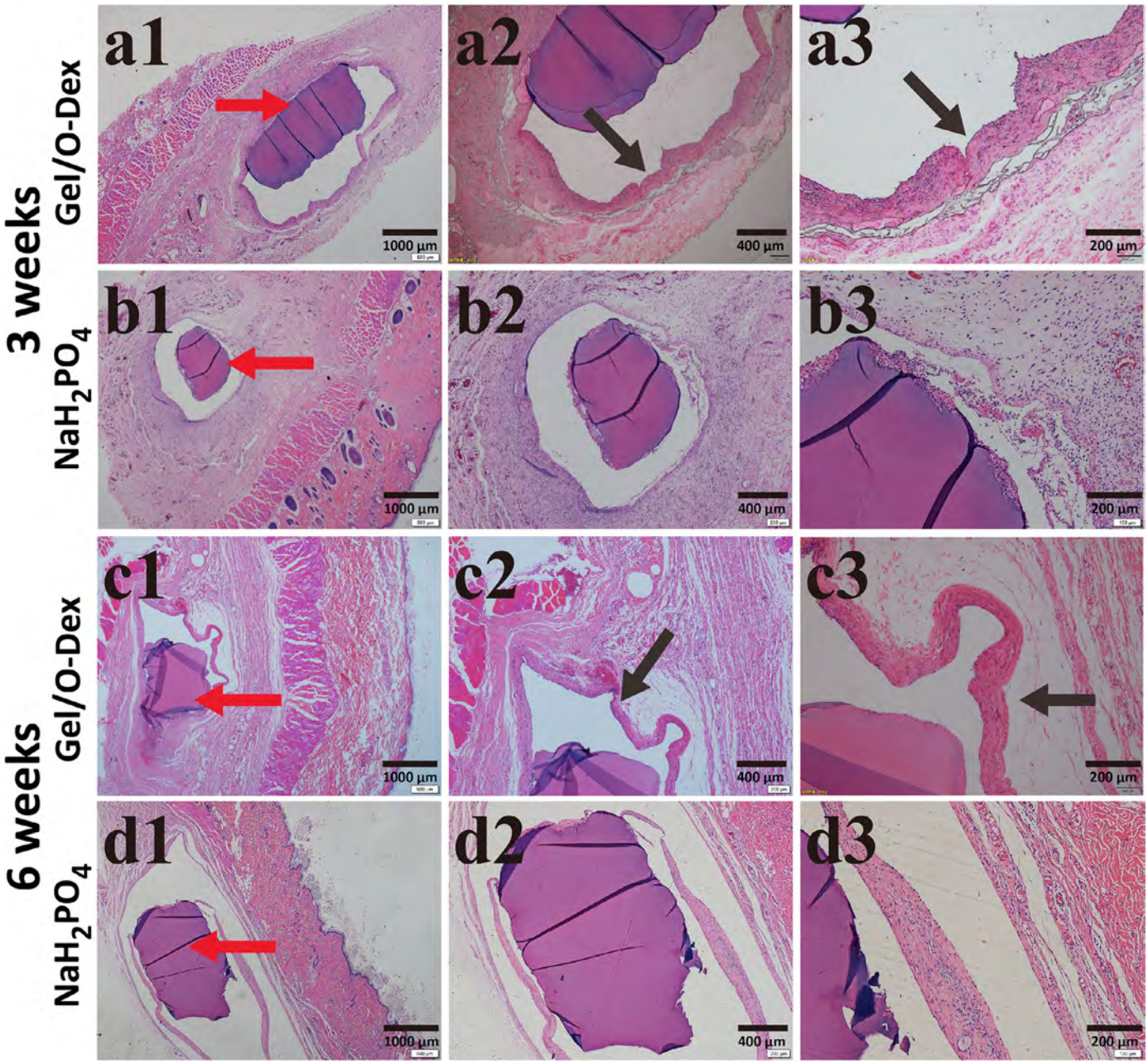

Fig. 7. Local tissue compatibility measurement of Hofmeister effect-enhanced Gel/O-Dex hydrogels *in vivo* at 3 weeks (a1-a3: Gel/O-Dex group; b1-b3: NaH_2PO_4 treated group) and 6 weeks (c1-c3: Gel/O-Dex group; d1-d3: NaH_2PO_4 treated group). (Red arrows: hydrogels; Black arrows: inflammatory zone of local foreign-body reaction).

Table 1
Atomic percentage results of Gel/O-Dex hydrogels untreated and treated with different concentrations of NaH_2PO_4 solutions.

Sample	Atomic percentage (%)				
	C	N	O	Na	P
Gel/O-Dex	65.38	10.56	22.91	0.52	0.63
Gel/O-Dex-10% NaH_2PO_4	55.29	7.68	30.89	2.39	3.76
Gel/O-Dex-20% NaH_2PO_4	44.46	8.79	37.61	4.34	4.80
Gel/O-Dex-30% NaH_2PO_4	32.38	3.10	49.72	6.82	7.98

was no significant difference in the high-resolution C 1s and N 1s XPS spectra between Gel/O-Dex and NaH_2PO_4 treated hydrogels. In the O 1s XPS spectra, there was significant difference between Gel/O-Dex and NaH_2PO_4 treated groups. The emission peak of O 1s can be typically decomposed into two individual peaks of C-O (532.6 eV) and C=O (531.4 eV) [40]. Compared with Gel/O-Dex group, NaH_2PO_4 treated hydrogels showed higher peak of C-O and lower peak of C=O. These results indicated that there was a significant decrease of aldehyde groups on the surface of hydrogel via Hofmeister effect treatment of $H_2PO_4^-$ anions. After Schiff base reaction, there were somewhat aldehyde groups unreacted in the hydrogel. The presence of residual aldehyde groups was not conducive to the proliferation of cells on the material [41,42]. Thus, the improved biocompatibility of Hofmeister effect-enhanced Gel/O-Dex hydrogels by $H_2PO_4^-$ ions was ascribed to the reduction of aldehyde groups. In addition, NaH_2PO_4 was an essential inorganic salt to maintain the normal physiological functions of cells. During the physical crosslinking process of Hofmeister effect, NaH_2PO_4 remaining on the surface also contributed to cell viability and improved the biocompatibility of the hydrogels. Thus,

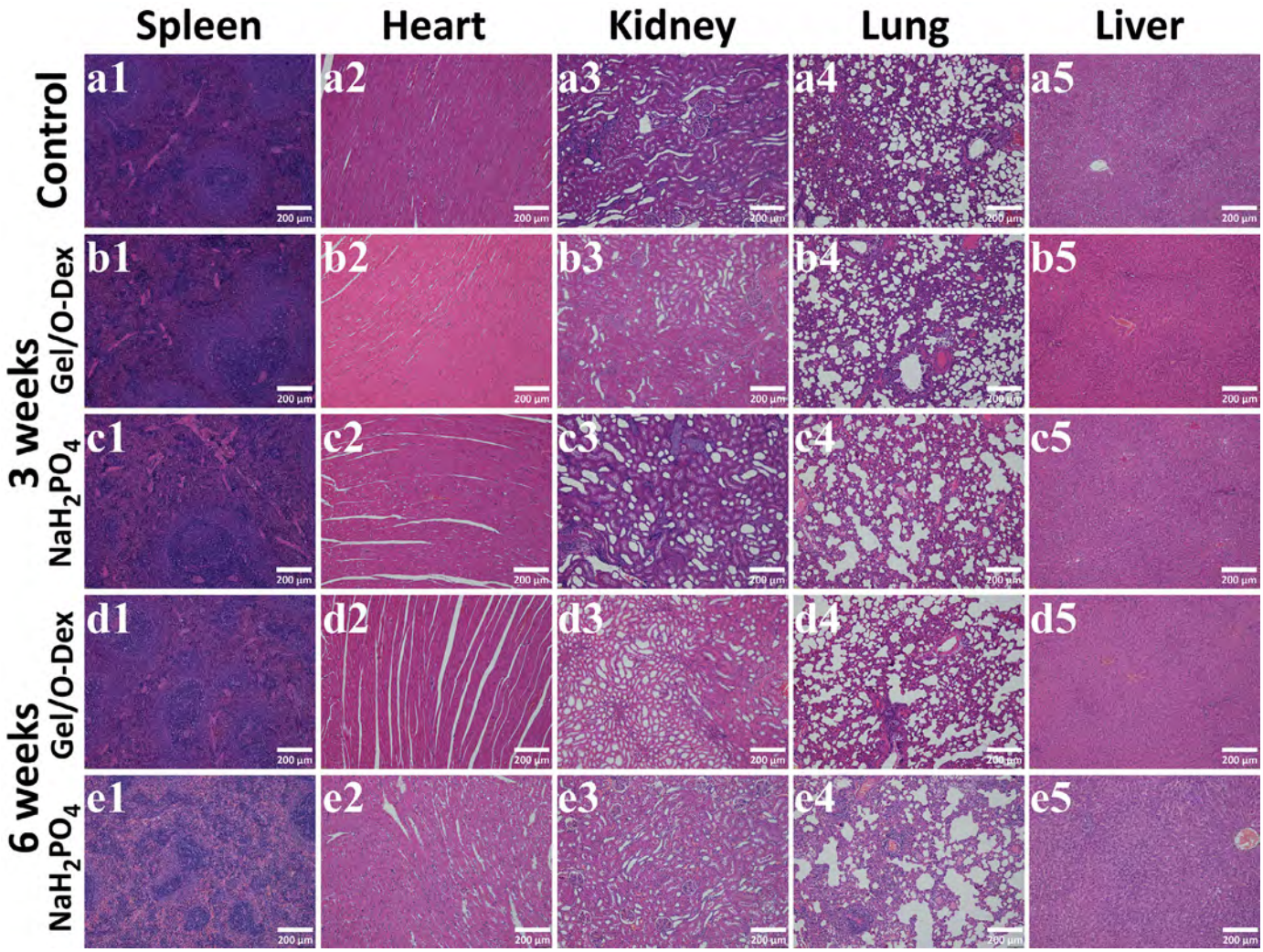

Fig. 8. Systemic toxicity measurement of Hofmeister effect-enhanced Gel/O-Dex hydrogels by $H_2PO_4^-$ ions *in vivo* at 3 weeks (a1-a5: Control group; b1-b5: Gel/O-Dex group; c1-c5: NaH_2PO_4 treated group) and 6 weeks (d1-d5: Gel/O-Dex group; e1-e5: NaH_2PO_4 treated group) through histological evaluation of spleen, heart, kidney, lung and liver.

XPS analysis showed that the improvement in biocompatibility of Hofmeister effect-enhanced hydrogels was due to the reduction of aldehyde groups and the residues of NaH_2PO_4. Hofmeister effect only induced the hydrophobic interactions and polymer chain entanglements without triggering any chemical reaction. We considered that aldehyde groups were embedded in the center of entangled polymer chains after Hofmeister effect of $H_2PO_4^-$ ions.

3.7. *Further biocompatibility assessment* in vivo *for Hofmeister effect-enhanced Gel/O-Dex hydrogels by $H_2PO_4^-$ ions*

In vivo assessment focused on local foreign-body reaction and systemic toxicity on vital organs. At 3 and 6 weeks after subcutaneous implantation into the dorsa of SD rats, all rats were alive and no skin necrosis or ulcers were observed. Histological staining of HE showed that there was a thin layer of inflammatory reaction zone between hydrogels and host tissue at 3 weeks. The reaction zone was stained as basophilic and infiltrated of inflammatory cells. Compared with Gel/O-Dex group, NaH_2PO_4 treated group showed a thinner tissue interfacial thickness between hydrogel and host tissue (Fig. 7 a1, b1). The number of infiltrated inflammatory cells in the Gel/O-Dex hydrogel group was also significantly higher than that in NaH_2PO_4 treated hydrogel group (Fig. 7 a3, b3). This was consistent with the results of *in vitro* cytotoxicity evaluation, indicating improved biocompatibility *in vivo* for Hofmeister effect-enhanced Gel/O-Dex hydrogels by $H_2PO_4^-$ ions. After 6 weeks, the infiltrated inflammatory cells decreased in the inflammatory reaction zone of two groups. There were no detectable inflammatory cells infiltrating in NaH_2PO_4 treated group while still some cells discoverable in Gel/O-Dex group.

In addition, *in vivo* assessment of systemic toxicity showed that both Hofmeister effect-enhanced and untreated Gel/O-Dex hydrogels presented a low level of systemic toxicity (Fig. 8). At 3 and 6 weeks there was no significant difference for histological evaluation of visceral organs including heart, liver, spleen, lung and kidney between the two groups. All the target organs were arranged in normal histological architectural structure by HE staining. Compared with normal visceral organs (Control group), no obvious dysfunction or malfunction of target organs was observed in all rats. We attributed these results to hydrogel degradation to naturally occurring amino acids and electrolyte ions.

3.8. *Accelerating wound healing of Hofmeister effect-enhanced Gel/O-Dex hydrogels by $H_2PO_4^-$ ions for full-thickness skin defects* in vivo

Fig. 9a was the schematic diagram of Hofmeister effect-enhanced Gel/O-Dex hydrogel repairing full-thickness skin defects

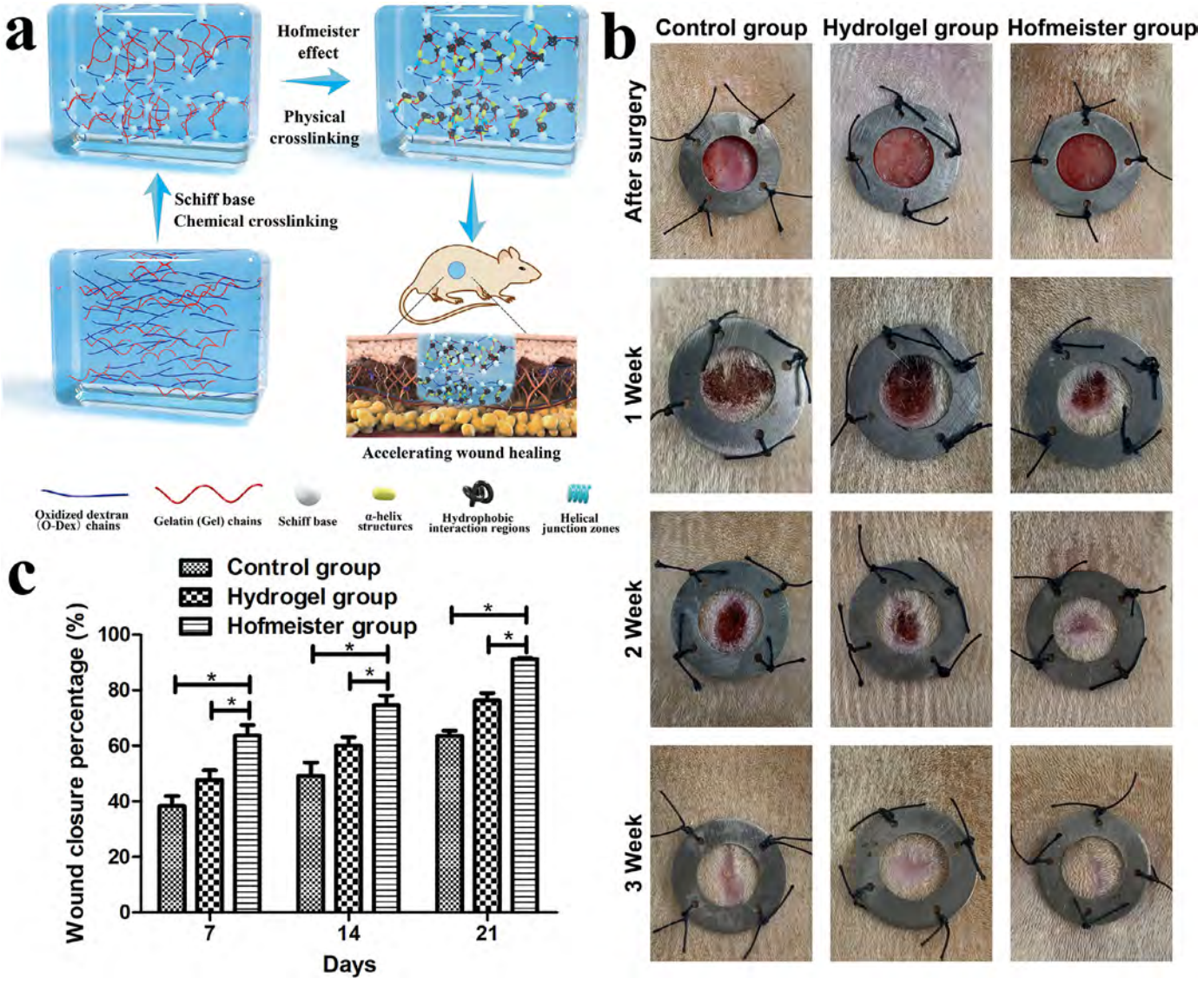

Fig. 9. (a) Schematic diagram of full-thickness skin defects in SD rat model treated with Hofmeister effect-enhanced Gel/O-Dex hydrogels. (b) Representative photographs of full-thickness skin defects in control group, hydrogel group and Hofmeister group after 7, 14, 21 days of wound healing. (c) Quantitative analysis of wound closure in control group, hydrogel group and Hofmeister group. The results showed that wound closure percentage treated with Hofmeister effect-enhanced Gel/O-Dex hydrogels by $H_2PO_4^-$ ions was significantly higher than other groups after 7, 14, 21 days.

in SD rats. The effect of hydrogel on wound healing was observed and evaluated at 7, 14, and 21 days. With the time of observation *in vivo*, the size of skin defects in all three groups decreased significantly, showing a process of wound healing (Fig. 9b). Compared with control group, full-thickness skin defects in hydrogel and Hofmeister groups exhibited accelerated wound healing process, indicating that Gel/O-Dex hydrogel and Hofmeister effect-enhanced Gel/O-Dex hydrogel had a beneficial effect on the wound healing. Especially for Hofmeister effect of $H_2PO_4^-$ ions, the regeneration rate of full-thickness skin defects was obviously faster. At 14 days, the defects in Hofmeister group were mainly healed due to the regenerative skin tissue while the wounds were still full-thickness in the other two groups (Fig. 9b). Quantitative analysis of wound closure percentage showed that the wound closure of the Hofmeister group was the highest at all time points (Fig. 9c). These indicated that Hofmeister effect-enhanced Gel/O-Dex hydrogels by $H_2PO_4^-$ ions accelerated the wound healing of full-thickness skin defects *in vivo*.

Then the histological morphology was analyzed among three groups by using HE (Fig. 10a) and Masson's trichrome staining (Fig. 10b). As observed from the HE staining, there was a clear boundary between the newly formed granulation tissue and the mature skin during the wound healing process. A large number of capillary vessels were clearly detected in the granulation tissue, which implied that the formed granulation tissue at the wound bed had not been developed into mature skin tissue. With the time of observation *in vivo*, the extent of granulation tissue in all three groups decreased gradually (Fig. 10a). The extent of granulation tissue was equal to the size of remaining wound area. After 3 weeks of wound healing, the size of remaining wound area in hydrogel group and Hofmeister group were less than that in control group, indicating that Gel/O-Dex hydrogel showed a beneficial effect on wound healing whether enhanced by Hofmeister effect or not (Fig. 10c). By contrast, with the enhancement of Hofmeister effect by $H_2PO_4^-$ ions, the wound healing efficiency was dramatically increased. As a result, the size of remaining wound area was less than 1 mm at 3 weeks (Fig. 10c) and the epidermal layer was completely formed in Hofmeister group (Fig. 10a). Compared with the other two groups, less granulation tissue was remained and more skin appendages were formed in Hofmeister group such as

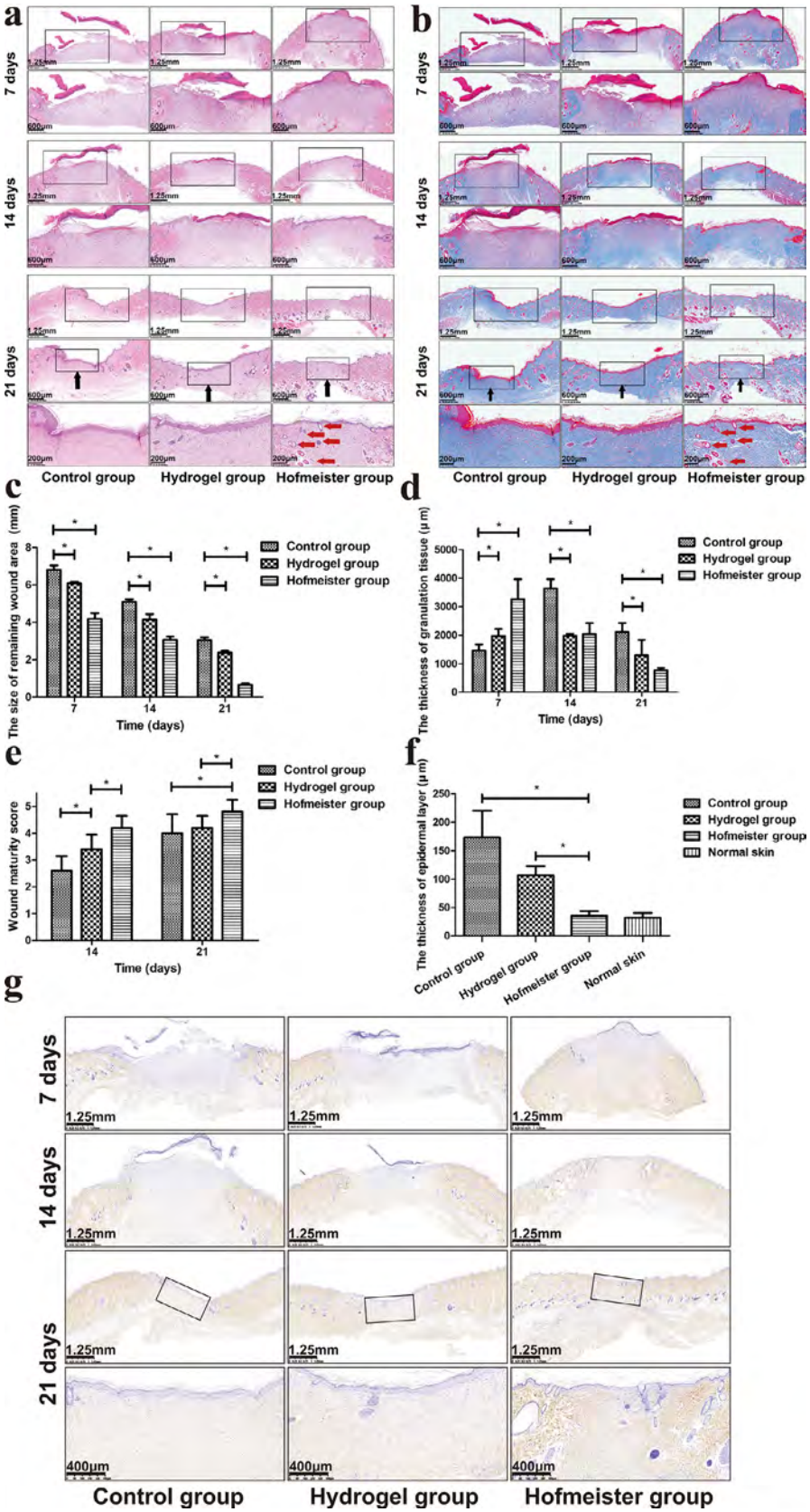

Fig. 10. (a) HE staining analysis of regenerated skin tissue in control group, hydrogel group and Hofmeister group after 7, 14, 21 days of wound healing; (b) Masson's trichrome staining analysis of regenerated skin tissue in control group, hydrogel group and Hofmeister group after 7, 14, 21 days of wound healing. (Black arrows and frames showed the regenerative area. Red arrows showed the regenerative blood vessels and skin appendages including hair follicles, sweat glands, and sebaceous glands.) (c) Quantitative analysis of the remaining wound area in control group, hydrogel group and Hofmeister group after 7, 14, 21 days of wound healing; (d) Quantitative analysis of granulation tissue thickness in control group, hydrogel group and Hofmeister group after 7, 14, 21 days of wound healing; (e) Quantitative assess of wound maturity in control group, hydrogel group and Hofmeister group after 14 and 21 days of wound healing; (f) Quantitative analysis of epidermal layer thickness in control group, hydrogel group and Hofmeister group at 21 days. (g) Immunochemical staining of type I collagen in control group, hydrogel group and Hofmeister group after 7, 14, 21 days of wound healing. (Frames showed the regenerative area.)

hair follicles, sweat glands, and sebaceous glands (Fig. 10b). These skin appendages endowed regenerated skin tissue more mature and showed that the granulation tissue successfully developed into mature skin tissue.

At the different phases of wound healing, granulation tissue played different function. At the early stage, granulation tissue was formed and increased, which allowed angiogenesis to initiate tissue blood perfusion and accelerated wound repair. At the late stage, the formation of granulation tissue was inhibited and remodeled that resulted in collagen deposition and differentiated into mature skin tissue. In the quantitative measurement of granulation tissue thickness, the thickness of granulation tissue of Hofmeister group was significantly higher than that of control group and hydrogel group at 7 days (Fig. 10d). We considered that the presence of more granulation tissue at the early stage provided more capillary vessels and proliferative cells to promote skin regeneration. Then granulation tissue was decreased in Hofmeister group. At 21 days, the thickness of granulation tissue of Hofmeister group was lower than that of other groups, indicating that the granulation tissue was successfully remodeled and developed into mature skin tissue (Fig. 10a).

During the process of wound healing, inflammation and proliferation are also important indicators that reflect the stage of the healing condition. The amounts of proliferative cells or inflammatory cells were closely associated with wound maturity. According to these two indicators, the wound maturity was divided into five levels, of which the wound gradually matured that level 1: no proliferative cells but highly inflammatory cells; level 2: mainly inflammatory cells; level 3: equal amounts of proliferative cells and inflammatory cells; level 4: mainly proliferative cells; level 5: differentiated cells. As shown by HE and Masson staining, there were proliferative cells to a certain extent and mainly inflammatory cells at 1 week. With the development of wound healing, proliferative cells gradually increased and differentiated into various types of skin mature cells. At 3 weeks, there were mainly differentiated cells to form skin appendages in Hofmeister group while there were proliferative and inflammatory cells infiltrating into the granulation tissue in other two groups. With the benefit of Hofmeister effect by $H_2PO_4^-$ ions, the wound maturity was dramatically enhanced that the regenerated skin showed identical histological morphology to normal skin. In the quantitative measurement of wound maturity, it was found that Hofmeister group had a higher wound maturity score than that of hydrogel group and control group (Fig. 10e).

Except for the wound maturity, collagen deposition is another necessary index during the remolding of granulation tissue. Thus, Masson's trichrome staining was furtherly analyzed to assess the condition of collagen deposition. As shown in Fig. 10b, the newly formed granulation tissue at 1 week was stained mainly in red and there was partially collagen deposition. Then the collagen was accumulated and gradually deposited in the granulation tissue to promote the healing of skin defects. At 3 weeks, the granulation tissues were all stained as blue in control group, hydrogel group and Hofmeister group. In the quantitative measurement of collagen deposition, the wound treated with Hofmeister effect-enhanced hydrogel exhibited a higher deposition percentage than that of control group and hydrogel group at 1 and 2 weeks. At 3 weeks, collagen deposition in the Hofmeister group was lower than that in the other two groups, because collagen was replaced by newly differentiated skin appendages. This was also supported by the assessment of wound maturity and the verification of histological morphology.

After the remolding of granulation tissue, epidermal layer was formed and appeared upon the dermis layer. The thickness of epidermal layer was correlated with the severity of scar formation. Compared with normal skin, increased epidermal thickness due to keratinocyte stimulation and abnormal differentiation, tended to result in scar hypertrophy. In the quantitative measurement of epidermal thickness, the regenerative epidermis of Hofmeister group exhibited the lower thickness than that of control group and hydrogel group at 3 weeks. There was no significant difference in epidermal thickness between Hofmeister group and normal skin, indicating that the use of Hofmeister effect-enhanced Gel/O-Dex hydrogel by $H_2PO_4^-$ ions had no adverse effect on scar formation (Fig. 10f). Moreover, the regenerated skin in Hofmeister group showed identical skin appendages consistent with normal skin, indicating that the granulation tissue was successfully remodeled and developed into normal skin tissue. In the tissue remodeling stage of wound healing, the granulation tissue formed in the early stage was replaced by type I collagen, ultimately resulting in the completion of wound healing. Compared with Gel/O-Dex hydrogel group, Hofmeister group showed an increased production of type I collagen in the immunochemical staining (Fig. 10g). Therefore, Gel/O-Dex hydrogel was confirmed to accelerate wound healing and improve the histological morphology of regenerated skin after the enhancement of Hofmeister effect by $H_2PO_4^-$ ions.

4. Conclusions

Schiff base reaction and Hofmeister effect were combined to prepare Hofmeister effect-enhanced Gel/O-Dex hydrogels with improved mechanical properties and biocompatibility for wound healing. Schiff base reaction is mild and simple, and Hofmeister effect just needs soaking in kosmotrope solutions. The combination of them greatly simplifies the preparation process for improving the properties of natural derived hydrogels. Hofmeister effect enhanced the mechanical properties by multiple times of ultimate stress of untreated Gel/O-Dex hydrogels through affecting the entanglements of protein chains and the stability of their secondary and tertiary structure. The pore size of morphology and compressive stress of Gel/O-Dex hydrogels treated with different anions was consistent with the order of Hofmeister series.

Especially for $H_2PO_4^-$ ions, both improved biocompatibility and mechanical properties were obtained by adding Schiff base chemical and ion physical crosslinking sites in synergy. The resulting hydrogels possessed elasticity, strong strength, recoverability and effectively dissipated the energy from large stress to resist fatigue. Simultaneously, the results showed that Hofmeister effect did not change chemical structure of polymer chains but just induced physical crosslinking domains of α-helix structures, hydrophobic interaction regions and helical junction zones among Gel molecular chains. Compared with untreated hydrogels, Hofmeister effect-enhanced hydrogels improved biocompatibility due to the reduction of aldehyde groups and the preservation of NaH_2PO_4 through physical crosslinking, which also dramatically promoted the wound healing in a full-thickness skin defects model.

Therefore, these findings indicate that Hofmeister effect-enhanced Gel/O-Dex hydrogels possess great potential for promoting wound healing in practical applications, and Hofmeister effect is proven as a promising approach to expand the further applications of natural derived hydrogels for tissue regeneration.

Declaration of Competing Interest

The authors declare no conflict of interest.

Acknowledgements

This work was financially supported by the National Natural Science Foundation of China (No. 81802144), the Research Projects of Shanghai Municipal Health Commission (No. 20194Y0316), Science and Technology Commission of Shanghai Municipality

(No. 20S31900900, 20DZ2254900), and Sino German Science Foundation Research Exchange Center (M-0263).

References

[1] J.Y. Sun, X. Zhao, W.R. Illeperuma, O. Chaudhuri, K.H. Oh, D.J. Mooney, J.J. Vlassak, Z. Suo, Highly stretchable and tough hydrogels, Nature 489 (2012) 133–136.

[2] Y.S. Zhang, A. Khademhosseini, Advances in engineering hydrogels, Science 356 (2017) eaaf3627.

[3] K.Y. Lee, D.J. Mooney, Hydrogels for tissue engineering, Chem. Rev. 101 (2001) 1869–1880.

[4] S. Huang, D.E. Ingber, The structural and mechanical complexity of cell-growth control, Nat. Cell Biol. 1 (1999) E131–E138.

[5] K.Y. Lee, J.A. Rowley, P. Eiselt, E.M. Moy, K.H. Bouhadir, D.J. Mooney, Controlling mechanical and swelling properties of alginate hydrogels independently by cross-linker type and cross-linking density, Macromolecules 33 (2000) 4291–4294.

[6] D.S. Bao, M.J. Chen, H.Y. Wang, J.F. Wang, C.F. Liu, R.C. Sun, Preparation and characterization of double crosslinked hydrogel films from carboxymethylchitosan and carboxymethylcellulose, Carbohydr. Polym. 110 (2014) 113–120.

[7] M. Mehrali, A. Thakur, C.P. Pennisi, S. Talebian, A. Arpanaei, M. Nikkhah, A. Dolatshahi-Pirouz, Nanoreinforced hydrogels for tissue engineering: biomaterials that are compatible with load-bearing and electroactive tissues, Adv. Mater. 29 (2017) 1603612.

[8] A. Nakayama, A. Kakugo, J.P. Gong, Y. Osada, M. Takai, T. Erata, S. Kawano, High mechanical strength double-network hydrogel with bacterial cellulose, Adv. Funct. Mater. 14 (2004) 1124–1128.

[9] S. Unterman, L.F. Charles, S.E. Strecker, D. Kramarenko, D. Pivoyarchik, E.R. Edelman, N. Artzi, Hydrogel nanocomposites with independently tunable rheology and mechanics, ACS Nano 11 (2017) 2598–2610.

[10] Y.Y. Jiang, Y.J. Zhu, H. Li, Y.G. Zhang, Y.Q. Shen, T.W. Sun, F. Chen, Preparation and enhanced mechanical properties of hybrid hydrogels comprising ultralong hydroxyapatite nanowires and sodium alginate, J. Colloid Interface Sci. 497 (2017) 266–275.

[11] Q. He, Y. Huang, S. Wang, Hofmeister effect-assisted one step fabrication of ductile and strong gelatin hydrogels, Adv. Funct. Mater. 28 (2018) 1705069.

[12] P. Jungwirth, P.S. Cremer, Beyond hofmeister, Nat. Chem. 6 (2014) 261–263.

[13] Y.J. Zhang, S. Furyk, D.E. Bergbreiter, P.S. Cremer, Specific ion effects on the water solubility of macromolecules: PNIPAM and the Hofmeister series, J. Am. Chem. Soc. 127 (2005) 14505–14510.

[14] L.M. Pegram, M.T. Record, Hofmeister salt effects on surface tension arise from partitioning of anions and cations between bulk water and the air-water interface, J. Phys. Chem. B 111 (2007) 5411–5417.

[15] X. Chen, S.C. Flores, S.M. Lim, Y.J. Zhang, T.L. Yang, J. Kherb, P.S. Cremer, Specific anion effects on water structure adjacent to protein monolayers, Langmuir 26 (2010) 16447–16454.

[16] J.M. Fox, K. Kang, W. Sherman, A. Heroux, G.M. Sastry, M. Baghbanzadeh, M.R. Lockett, G.M. Whitesides, Interactions between Hofmeister anions and the binding pocket of a protein, J. Am. Chem. Soc. 137 (2015) 3859–3866.

[17] Y. Li, C. Liu, Y. Tan, K. Xu, C. Lu, P. Wang, *In situ* hydrogel constructed by starch-based nanoparticles via a Schiff base reaction, Carbohydr. Polym. 110 (2014) 87–94.

[18] J. Shi, W. Guobao, H. Chen, W. Zhong, X. Qiu, M.M.Q. Xing, Schiff based injectable hydrogel for *in situ* pH-triggered delivery of doxorubicin for breast tumor treatment, Polym. Chem. 5 (2014) 6180–6189.

[19] L. Wang, F. Deng, W. Wang, A. Li, C. Lu, H. Chen, G. Wu, K. Nan, L. Li, Construction of injectable self-healing macroporous hydrogels via a template-free method for tissue engineering and drug delivery, ACS Appl. Mater. Interfaces 10 (2018) 36721–36732.

[20] J. Liu, J. Li, F. Yu, Y.X. Zhao, X.M. Mo, J.F. Pan, *In situ* forming hydrogel of natural polysaccharides through Schiff base reaction for soft tissue adhesive and hemostasis, Int. J. Biol. Macromol. 147 (2020) 653–666.

[21] J. Li, F. Yu, G. Chen, J. Liu, X.L. Li, B. Cheng, X.M. Mo, C. Chen, J.F. Pan, Moist-retaining, self-recoverable, bioadhesive, and transparent *in situ* forming hydrogels to accelerate wound healing, ACS Appl. Mater. Interfaces 12 (2020) 2023–2038.

[22] K.S.W. Sing, D.H. Everett, R.A.W. Haul, L. Moscou, R.A. Pierotti, J. Rouquerol, T. Siemieniewska, Reporting physisorption data for gas solid systems with special reference to the determination of surface-area and porosity (Recommendations 1984), Pure Appl. Chem. 57 (1985) 603–619.

[23] M. Kruk, M. Jaroniec, Gas adsorption characterization of ordered organic-inorganic nanocomposite materials, Chem. Mater. 13 (2001) 3169–3183.

[24] L. Fan, H. Yang, J. Yang, M. Peng, J. Hu, Preparation and characterization of chitosan/gelatin/PVA hydrogel for wound dressings, Carbohydr. Polym. 146 (2016) 427–434.

[25] T.C. Lai, J. Yu, W.B. Tsai, Gelatin methacrylate/carboxybetaine methacrylate hydrogels with tunable crosslinking for controlled drug release, J. Mater. Chem. B 4 (2016) 2304–2313.

[26] Y.R. Choi, E.H. Kim, S. Lim, Y.S. Choi, Efficient preparation of a permanent chitosan/gelatin hydrogel using an acid-tolerant tyrosinase, Biochem. Eng. J. 129 (2018) 50–56.

[27] Y. Zhang, P.S. Cremer, The inverse and direct Hofmeister series for lysozyme, Proc. Natl. Acad. Sci. USA 106 (2009) 15249–15253.

[28] S.H. Jung, K.Y. Kim, J.H. Lee, C.J. Moon, N.S. Han, S.J. Park, D. Kang, J.K. Song, S.S. Lee, M.Y. Choi, J. Jaworski, J.H. Jung, Self-assembled Tb(3+) complex probe for quantitative analysis of atp during its enzymatic hydrolysis via time-resolved luminescence *in vitro* and *in vivo*, ACS Appl. Mater. Interfaces 9 (2017) 722–729.

[29] R. Arumugaperumal, V. Srinivasadesikan, M.V. Ramakrishnam Raju, M.C. Lin, T. Shukla, R. Singh, H.C. Lin, Acid/base and H_2PO_4– controllable high-contrast optical molecular switches with a novel BODIPY functionalized [2]rotaxane, ACS Appl. Mater. Interfaces 7 (2015) 26491–26503.

[30] J. Li, Y. Chen, Y. Yin, F. Yao, K. Yao, Modulation of nano-hydroxyapatite size via formation on chitosan-gelatin network film *in situ*, Biomaterials 28 (2007) 781–790.

[31] D. Chandler, Interfaces and the driving force of hydrophobic assembly, Nature 437 (2005) 640–647.

[32] F.N. Fu, D.B. Deoliveira, W.R. Trumble, H.K. Sarkar, B.R. Singh, Secondary structure estimation of proteins using the amide-iii region of fourier-transform infrared-spectroscopy - application to analyze calcium binding-induced structural-changes in calsequestrin, Appl. Spectrosc. 48 (1994) 1432–1441.

[33] S.W. Cai, B.R. Singh, Identification of beta-turn and random coil amide III infrared bands for secondary structure estimation of proteins, Biophys. Chem. 80 (1999) 7–20.

[34] S.W. Cai, B.R. Singh, A distinct utility of the amide III infrared band for secondary structure estimation of aqueous protein solutions using partial least squares methods, Biochemistry 43 (2004) 2541–2549 Us.

[35] A. Chapiro, N. Schmitt, Préparation d'hydrogels par radiolyse de solutions de poly(vinyl-1-imidazole) en présence d'un monomère, Eur. Polym. J. 33 (1997) 1341–1344.

[36] X.T. Wang, C.Z. Wei, B. Cao, L.X. Jiang, Y.T. Hou, J. Chang, Fabrication of multiple-layered hydrogel scaffolds with elaborate structure and good mechanical properties via 3D printing and ionic reinforcement, ACS Appl. Mater. Interfaces 10 (2018) 18338–18350.

[37] S.Y. Tang, K. Liu, J.S. Chen, Y.Z. Li, M.X. Liu, L. Lu, C.R. Zhou, B.H. Luo, Dual-cross-linked liquid crystal hydrogels with controllable viscoelasticity for regulating cell behaviors, ACS Appl. Mater. Interfaces 14 (2022) 21966–21977.

[38] K. Prusty, S.K. Swain, Nano silver decorated polyacrylamide/dextran nanohydrogels hybrid composites for drug delivery applications, Mater. Sci. Eng. C Mater. Biol. Appl. 85 (2018) 130–141.

[39] Y.C. Chang, C.J. Lee, L.W. Wang, Y.H. Wang, Highly uniform resistive switching properties of solution-processed silver-embedded gelatin thin film, Small 14 (2018) e1703888.

[40] G.P. López, D.G. Castner, B.D. Ratner, XPS O 1s binding energies for polymers containing hydroxyl, ether, ketone and ester groups, Surf. Interface Anal. 17 (1991) 267–272.

[41] V.J. Feron, H.P. Til, F. de Vrijer, R.A. Woutersen, F.R. Cassee, P.J. van Bladeren, Aldehydes: occurrence, carcinogenic potential, mechanism of action and risk assessment, Mutat. Res./Genet. Toxicol. 259 (1991) 363–385.

[42] U.J. Kim, Y.R. Lee, T.H. Kang, J.W. Choi, S. Kimura, M. Wada, Protein adsorption of dialdehyde cellulose-crosslinked chitosan with high amino group contents, Carbohydr. Polym. 163 (2017) 34–42.